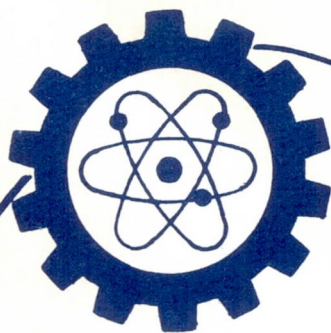


NG3- 22174

578599
P.88



EXOTECH
INCORPORATED

OTS PRICE

XEROX	\$	_____
MICROFILM	\$	_____

4208 WHEELER AVENUE • ALEXANDRIA, VIRGINIA



INVESTIGATION OF PRECESSION CONTROL
AND ORBIT MAINTENANCE SYSTEMS
FOR ROTATING SPACE STATIONS

SUMMARY REPORT

to

The National Aeronautics and Space Administration

Contract No. NAS w-543

Report TR-002

May 1963

EXOTECH INCORPORATED
4208 Wheeler Avenue
Alexandria, Virginia

Telephone 836-1972

TABLE OF CONTENTS

	Page
I Introduction	1
II Analysis of Disturbing Torques and Thrust Requirements	3
A. Objectives and Basic Assumptions	3
B. Comparison of the Relative Magnitude of Disturbing Torques and Thrust Requirements	4
C. Gravity Gradient Torques	10
D. Station Angular Misalignment	12
E. Estimates of Propellant Weight	13
F. Methods of Thrust Application	17
III Design Studies of an Electrically-Heated Pulse Rocket (Ohmjet) Thrust System	19
A. General Discussion	19
B. Description of Carbon Dioxide Recovery Systems	19
C. Sizing of System Components	26
D. Electrical Power Requirements	32
E. Weight Estimates	38
F. Discussion	38
IV Design Studies of a Solar-Heated Pulse Rocket (Heliojet) Thrust System	42
A. Design Requirements	42
B. Optical Design Considerations	44
C. Receiver Heat-up Rates	48
D. Transient Heat Transfer Analysis	51
E. Heliojet Configuration	52
F. Weight Estimates	53
G. Conclusions	55
V Experimental Testing of Ohmjet Thrust Unit	57
A. Test Objectives	57
B. Description of Ohmjet Unit	57
C. Discussion of Ohmjet Testing Under Pulsed Operating Conditions	59
D. Discussion of Ohmjet Testing Under Steady State Operating Conditions	64

	page
VI Conclusions	70
VII Recommendations	72
References	73
Appendix A - Transient Heat Transfer Analysis of the Heliojet	74

LIST OF FIGURES

<u>Figure</u>		<u>Page</u>
II-1	Error Angle vs Time, as Produced by Secular Component of Gravity Gradient	14
II-2	Sun Orientation Error Angle Produced by Gravity Gradient (Secular Component) in One Quarter Orbit (22.5 Min.)	15
II-3	Efficiency of Propellant Utilization vs Fractional Duty Cycle	16
III-1	Schematic Diagram of CO ₂ Recovery, Pressurization and Storage System, Method I	20
III-2	Schematic Diagram of CO ₂ Recovery System for Direct Use of CO ₂ From Molecular Sieve Bed, Method II	21
III-3	Schematic Diagram Showing Thrust Cycle to Accomplish Orbit Maintenance	23
III-4	Adsorption Isotherms for CO ₂ in Linde Type 5A Molecular Sieve Pellets	24
III-5	Temperature History of Molecular Sieve Bed During Cooling Cycle	29
III-6	Power Requirements, Method I, Duty Cycle 1	33
III-7	Power Requirements, Method I, Duty Cycle 2	34
III-8	Power Requirements, Method II, Duty Cycle 1	35
III-9	Power Requirements, Method II, Duty Cycle 2	36
IV-1	Geometry of Heat Exchanger Tube	45
IV-2	Solar Collector Geometry	47
IV-3	Cavity Receiver Heat-up Rates for Heliojet	50
IV-4	Configuration of Heliojet Thrust Unit	54
V-1	Ohmjet Thrust Unit	58
V-2	Ohmjet Thrust Test Stand	60
V-3	Photograph of Ohmjet Thrust Test Stand	61
V-4	Thrust-Time Record at 125 psig Regulated Pressure	62
V-5	Thrust-Time Record at 150 psig Regulated Pressure	62

LIST OF FIGURES (CONT'D)

<u>Figure</u>		<u>Page</u>
V-6	Static Load Calibration of Test Stand	63
V-7	Ohmjet CO ₂ Discharge Temperature as a Function of Power Input & Inlet Pressure	67
V-8	Heat Transfer Coefficient vs Mass Velocity for Ohmjet Helical Heater	69
A-1	Tube Geometry for Heat Transfer Analysis	76
A-2	Heliojet Gas Exit Temperature Variation With Time	80
A-3	Heliojet Average Wall Temperature Variation With Time	81
A-4	Comparison of Solutions to Transient Heat Transfer Equations	82

ABSTRACT

An analysis is presented of the thrust requirements to compensate for gravity gradient torques and aerodynamic drag and to accomplish annual precession of rotating manned space stations. Analysis and design studies of electrically heated and solar-heated reaction control systems which use carbon dioxide as the working fluid are reported. Experimental data obtained by transient and steady state performance testing of an Ohmjet electrically-heated pulse rocket are discussed. Conclusions and recommendations are presented regarding the applicability of Ohmjet and Heliojet thrust systems for reaction control of manned space stations.

I INTRODUCTION

The objective of this program has been to conduct analytical and design studies to aid in the selection and design of precession control and orbit maintenance systems for a rotating space station, utilizing electrically-heated and solar-heated pulse rockets. Also experiments were conducted to determine the performance parameters of an Ohmjet electrical resistance-heated rocket of a type applicable for precession control.

The effort was divided into the following five tasks:

- (a) Analysis and design studies to determine the required performance parameters for thrust producing systems.
- (b) Analysis of the design parameters for an Ohmjet thrust system.
- (c) Analysis of the design parameters for a solar-heated (Heliojet) thrust system.
- (d) Experimental performance evaluation tests of a prototype Ohmjet thrust unit which had been previously designed and fabricated by Exotech Incorporated.
- (e) Development and improvement of the Ohmjet thrust unit.

The general reasons for interest in the application of electrically-heated and solar-heated pulse rockets for attitude control and orbit maintenance of manned space stations are:

1. The use of waste carbon dioxide from a manned spacecraft for reaction control would reduce or eliminate the requirement for additional chemical propellants. However, the availability of CO_2 for thrust production would be contingent on a decision not to regenerate CO_2 into oxygen because of system considerations such as short mission duration or lack of reliable oxygen regeneration equipment.
2. The disturbing torques and forces on a manned space station include a fairly steady "base load" requirement to compensate for gravity gradient torques and aerodynamic drag and to provide precession at a steady rate of one revolution per year for sun-orientation. These base load requirements can potentially be met by using waste carbon dioxide which would be generated by the crew at a fairly constant rate. Peak loads on the attitude control system which would be imposed by docking forces, motion of the crew, etc. could be met by a separate system incorporating chemical rockets and flywheels or gyros.

3. The concept of using electrical or solar energy to heat a working fluid for reaction propulsion has broad potential for application to spacecraft if waste fluids can be used effectively or if a low molecular weight propellant such as hydrogen or ammonia can be used, so that the specific impulse may exceed that attainable by chemical rockets. The technology of such devices needs further development.

It is hoped that the analysis, design and experimental efforts reported herein will aid in defining the directions for future development of the technology of reaction control systems using pulsed operation of electrically-heated and solar-heated thrust devices.

II ANALYSIS OF DISTURBING TORQUES AND THRUST REQUIREMENTS

A. Objectives and Basic Assumptions

The purpose of this analysis is to provide a basis for the preliminary design of the reaction control system for a rotating sun-oriented space station. The function of the reaction control system is to point the spin-axis toward the sun and to compensate for aerodynamic drag in order to maintain orbit altitude.

Wherever possible the analysis is made general enough to render it applicable over a range of orbit and station parameters. For the purpose of making numerical estimates, however, the following specific values are used:

Circular Orbit Altitude	300 nautical miles
Orbit Inclination	30 degrees
Spin Axis Moment of Inertia	$I_Z = 1.5 \times 10^7 \text{ slug-ft}^2$
Transverse Moments of Inertia	$I_X = I_Y = 1.05 \times 10^7 \text{ slug-ft}^2$
Station radius (maximum moment arm for thrust application)	75 feet
Spin rate	3 RPM

The reaction control system must have sufficient capacity to counter all external disturbances which alter station momentum (both linear and angular). These disturbances can be categorized as follows:

I. Orbit Maintenance

- (a) Aerodynamic drag
- (b) Solar radiation-pressure (negligible for space stations)

II. Attitude Control (Sun-Orientation)

- (a) Yearly precession around the sun
- (b) Gravity-Gradient
- (c) Aerodynamic torques
- (d) Solar-radiation pressure torques
- (e) Interaction with earth's magnetic field
- (f) Meteoroid impacts

The relatively low altitude and the fact that this is a spinning station makes some of the above disturbances dominant in comparison to the other. It was thus found that the largest single source of disturbance is that due to gravity gradient torques; the second largest disturbance source is that due to the yearly motion of the earth around the sun. The amount of average thrust required for orbit control purposes was found to be comparable to the average thrust needed to accomplish annual precession.

The major disturbing torque produced by gravity gradient and the torque required to precess the station spin axis by one revolution per year (the annual precession torque) are both amenable to detailed analysis. In both cases, orbit and station design parameters entering into the analysis are known and remain relatively constant and the analysis can be based on well established laws of mechanics. Therefore the analysis can be rigorous and the results can have general utility in defining the predominant long term (secular) torque and thrust requirements. The analysis was intentionally conducted in this general manner in order to estimate "base load" requirements and to avoid consideration of short time transient disturbing effects such as docking loads, motion of crew, etc. which can be separately counteracted and which involve detailed system and operational assumptions.

B. Comparison of the Relative Magnitude of Disturbing Torques and Thrust Requirements

It is convenient to use the annual precession torque as a reference and to compare all other torques with it. The torques are expressed in terms of the average thrust required at a moment arm of 75 feet from the center of mass.

(a) Annual Precession Torque

Motion of the earth and therefore the space station around the sun introduces the requirement that the station axis of symmetry, which is also the spin axis, must precess in inertial space at a rate of one revolution per year in order to maintain sun orientation which would permit use of solar power and simplify thermal control. The magnitude of the average torque needed to produce this annual precession is given by the gyroscope equation:

$$T_P = I_Z \Omega_Z \omega$$

Ω_Z = spin rate about sun-pointing axis

ω = 1 revolution per year

For the numerical values previously defined

$$T_P = 0.94 \text{ lb-ft}$$

and the average thrust at a moment arm of 75 ft is

$$F_P = 0.0125 \text{ lbs}$$

The utility of the precession torque as a reference stems from the fact that it is independent of orbit parameters, i.e. altitude, or inclination, and that it is constant with time.

It is noted that the annual precession torque vector must lie in the ecliptic plane and be perpendicular to the earth-sun line in order to produce precession around an axis perpendicular to the ecliptic plane. Therefore thrust must be applied toward or away from the sun at points above or below the ecliptic plane passing through the station center of mass. Since the station is rotating around the earth-sun line, it is impossible to produce a steady annual precession torque by continuous operation of a thrust device which is fixed to the space station. Therefore the thrust must actually be applied in pulses while the thrust device is above or below the ecliptic plane.

(b) Gravity Gradient Torques

We consider next the magnitude of gravity gradient torques. As derived in the course of this study, the average value over any one orbit of the secular component of the gravity gradient torque is given by the expression

$$T_G = \frac{3\pi^2}{P_0^2} (I_Z - I_X) D_S \quad (2)$$

where P_0 = orbital period

D_S is a function of orbital parameters and its value depends upon initial launch conditions. In general, D_S varies between zero and 1 with a period of about 54 days. However, for the assumed orbit inclination of 30° it is always larger than zero. For the present purpose of comparing magnitudes we will assume an average value of 0.6.

As shown in reference 1, for a spinning body in which $I_Z > I_X$, stability of rotation requires that I_Z be about 1.5 to 2 times larger than I_X .

We assume

$$I_Z = 2 I_X$$

Hence

$$I_Z - I_X = (1/2) I_Z \quad (3)$$

To compare gravity-gradient torques with the precession torque we evaluate their ratio:

$$\frac{T_G}{T_P} = \frac{3\pi^2}{2P_0^2} \frac{D_S}{Z} \quad (4)$$

For P_0 in minutes and Ω_Z in RPM, equation (4) becomes

$$\frac{T_G}{T_P} = (2 \times 10^5) \frac{D_S}{P_0^2 \Omega_Z} \quad (5)$$

Evidently, the relative magnitude of these torques is influenced only by the spin rate and orbital period. For the particular case considered here, P_0 varies only slightly with altitude, i.e., it is 95 minutes at 300 n.miles and 92 minutes at 200 n.miles. Using $\Omega_Z = 3$ RPM we get a maximum ratio (for $D_S = 1$) of:

$$\left(\frac{T_G}{T_P} \right)_{\max} = 7.27$$

and an average ratio (for $D_S = 0.6$) of:

$$\left(\frac{T_G}{T_P} \right)_{\text{average}} = 4.36$$

Thus, the secular gravity gradient torque is substantially larger than the torque required for annual precession.

It is worth noting that the above will be true for all practical configurations of a rotating sun-oriented station where the function of rotation is to provide artificial gravity. For example, as a limiting case, assume that it is desired to provide a full 1g of centipetal acceleration at a radius of only 32 feet. This would require a spin rate

of 10 RPM and for the same range of orbital altitudes the average value of the secular gravity gradient torques would be 1.32 times as large as the orbital precession torque. This ratio for $D_S = 1$ would be 2.2. Hence the validity of the basic conclusion is not significantly affected by changes in station design parameters.

(c) Orbit Control

We consider next the average thrust required to maintain orbit altitude. Although for completeness, radiation-pressure was listed as a source of disturbance, it is of no practical relevance because in the altitude range considered it is at least two orders of magnitude smaller than aerodynamic pressure. The principal cause of orbit decay is therefore air drag.

It is assumed that the drag force is directed along the negative velocity vector and equals

$$F_D = (1/2) C_D A_P \rho(h) V^2 \quad (6)$$

A_P = projected area normal to velocity vector

$\rho(h)$ = air density as a function of altitude

V = satellite velocity

We will assume free molecular flow and completely diffuse reflection of molecules rebounding from the surface. Under these conditions, and neglecting the thermal velocity of impinging molecules by comparison with the orbital station velocity, the drag coefficient is:

$$C_D = 2$$

To evaluate the projected area, we assume the station to be an annular disk of inner radius r_1 and outer radius r_2 , with its axis pointing toward the sun.

Denoting by A the area of the ring:

$$A = \pi(r_2^2 - r_1^2) \quad (7)$$

The projected area A_P in the direction of the velocity vector varies from zero to A over each quarter orbit because of the variation of the angle ϕ between the sun line and the velocity vector. For a circular orbit in the ecliptic plane:

$$A_P = A \cos \phi$$

The average value of A_p for a nearly circular orbit is:

$$A_{PA} = \frac{2}{\pi} A \int_0^{\pi/2} \cos \phi d\phi = \frac{2}{\pi} A \quad (9)$$

The average value of the drag force therefore becomes:

$$F_D = 2 (r_2^2 - r_1^2) \rho(h) v^2 \quad (10)$$

The largest uncertainty in estimating the drag force is due to the lack of definitive data on the daily average of air density at the altitudes of interest. As shown in reference (2) there is a spread of one order of magnitude in the air density values reported by various investigators for any one altitude. We use data based on reference (3), viz.

at 200 n.miles	$\rho \approx 3 \times 10^{-14} \text{ gm/cm}^3$
at 300 n.miles	$\rho \approx 3 \times 10^{-15} \text{ gm/cm}^3$

To estimate F_D , we use $r_2 = 75 \text{ ft}$, $r_1 = 65 \text{ ft}$. The average drag force is then found to be:

$h = 200 \text{ n.miles}$	$F_D = 0.083 \text{ lbs}$
$h = 300 \text{ n.miles}$	$F_D = 0.008 \text{ lbs}$

The average thrust to provide annual precession torques was previously found to be 0.0125 lbs. At an altitude of 300 n.miles the average thrust required to compensate for drag is therefore approximately equal to that needed to provide annual precession torque. However at 200 n.miles the drag effect is about 6.6 times larger and is therefore comparable to the peak values of gravity gradient torque, with respect to thrust requirement.

(d) Aerodynamic Torques

The preceding calculations of air drag can be used to estimate aerodynamic torques on the station. These would be due to a displacement Δr of the center of pressure from the center of mass and could be calculated from

$$T_D = F_D \cdot \Delta r \quad (11)$$

The value of Δr depends upon the size and geometry of the station and might be expected to be a few percent of the maximum radius, say:

$$\Delta r = 0.02 r_{\text{max}}$$

Hence

$$T_D = 0.02 F_D \cdot r_{\max} \quad (13)$$

Using equation (13) the comparison between annual precession torque and aerodynamic torque is as follows:

$$h = 300 \text{ n.miles} \quad \frac{T_D}{T_P} = 0.013$$

$$h = 200 \text{ n.miles} \quad \frac{T_D}{T_P} = 0.133$$

In either case, therefore, aerodynamic torques are substantially smaller than the required annual precession torque.

(e) Solar Radiation-pressure

As previously noted, solar radiation pressure is a few orders of magnitude smaller than aerodynamic pressure at the altitudes of interest. Hence, the effect becomes negligible by comparison with the other disturbing torques.

(f) Magnetic Interaction Torque

Since the magnitude of torque due to interaction with the earth's magnetic field depends upon the amount of magnetic materials in the station and the size and location of current loops, it can be assumed that precaution in design will keep these torques down to a low value. In general, these torques may be expected to be less than the aerodynamic torques, unless the station were specifically designed to use magnetic torques for control.

(g) Meteoroid Impacts

Lack of definitive data on meteoroid fluxes makes a realistic estimate difficult. However, based on prior analyses, it is believed that the torque requirements to compensate for meteoroid impacts will be negligible.

(h) Summary

The data developed above can be summarized in tabular form by showing the various average thrust levels as a fraction of the thrust needed to provide for annual precession.

Disturbance	Fraction of Annual Precession Thrust	
	h = 200 n.miles	h = 300 n.miles
Annual Precession	1	1
Aerodynamic Drag Force	6.6	0.64
Gravity Gradient Torque	4.5	4.36
Aerodynamic Torque	0.13	0.01
Magnetic Interaction Torque	0.2	0.2
Meteoroid Impact		
Radiation-Pressure Torque		
TOTALS	12.43	6.21

The totals shown above indicate that propellant requirements would be twice as large at 200 n.miles as compared to an orbital altitude of 300 n.miles. It is to be noted, however, that since the difference is caused primarily by the increased drag on the station, and since this estimate is based upon assumed values of density which are not very reliable, the factor of two indicated above is rather uncertain. Even though there is no agreement on the absolute value of air density at any one altitude, it is probable that the average density changes by about one order of magnitude between 200 and 300 n.miles. Hence, from the point of view of minimizing propellant weight for reaction control purposes, the orbital altitude should be 300 n.miles. Assuming that this would be the design choice, the largest single source of torque would be gravity gradient. Furthermore, gravity gradient and annual precession torques would account for at least 87% of the total propellant weight required, even if no attempt were made to use attitude control impulses to accomplish drag compensation at the same time.

C. Gravity Gradient Torques

A preliminary analysis of gravity gradient torques on a rotating, sun-oriented station is reported in Topical Report TR-001, (Ref. 4). The following is intended to summarize Ref. 4 and the additional analyses performed during the program.

It is estimated that a saving of about 20% in propellant consumption can be achieved by applying the control impulses with a single nozzle at a time when station rotation has brought this nozzle to an angular position in the plane of the station which is 90 degrees away from the axis about which the torque is to act. From the point of view of evaluating disturbance torques, this implies that only the total torque magnitude is relevant, regardless of where this vector might lie in the plane of the station. The analysis of gravity gradient torques was therefore made in terms of the total torque magnitude, rather than separate components in the plane of, and perpendicular to, the ecliptic plane.

The instantaneous value of the total gravity gradient torque is given by

$$J_T = \frac{3}{2} \frac{GM}{R_0^3} (I_Z - I_X) \sin 2\theta_3 \quad (14)$$

GM = gravitational constant for the earth

R_0 = orbital radius

I_Z = moment of inertia about spin axis

$I_X = I_Y$ = moment of inertia about axes in the plane of the station

θ_3 = angle between the sun-pointing spin-axis and earth's radius vector.

Since θ_3 varies with the instantaneous value of the various orbital parameters, the total gravity-gradient torque will be time varying. However, because the period of the satellite in its orbit around the earth is much shorter than the period of the orbit around the sun, the gravity gradient torque can be defined as a product of two terms, one of which is constant over any one orbit. Integrating the torque over a complete orbit, the following expression was derived for the angular momentum per orbit due to the total gravity gradient torque:

$$H_T = \frac{12\pi}{P_0} (I_Z - I_X) f(D) \quad (\text{per orbit}) \quad (15)$$

where

$$f(D) = D + \frac{1}{2}(1-D^2) \ln \left(\frac{1+D}{1-D} \right)$$

$$D = \sqrt{1 - \sin^2 i \sin^2 \psi}$$

i = angle of inclination of the orbit plane to the ecliptic plane at launching and which changes slowly as orbit regression occurs.

ψ = angle between the spin axis and the intersection of the orbit plane with the ecliptic plane, which also varies with time.

The parameter $f(D)$ is a function of the various orbital parameters and changes slowly with time. Its definition requires a knowledge of orbit inclination, altitude and time of launch. If these parameters are specified, the propellant consumption required for torque compensation, or the station angular misalignments can be evaluated as a function of time.

For the assumed orbital parameters, the maximum value of $f(D)$ is 1.2. Although theoretically $f(D)$ can also reach zero (when i and ψ are 90°), this could not be the case for the assumed value of $i = 30^\circ$.

A similar approach was taken to evaluate only the secular component of the total gravity gradient torque. Angular momentum over one orbit is in this case given by

$$H_S = \frac{3\pi^2}{P_0} (I_Z - I_X) D_S \quad (\text{per orbit}) \quad (16)$$

where

$$D_S = 2 \sin i \sin \psi \sqrt{1 - \sin^2 i \sin^2 \psi}$$

D_S is also a function of the time varying orbital parameters, but differs from $f(D)$. The maximum value of D_S is 1 and, for the assumed value of $i = 30^\circ$, will always be larger than zero.

D. Station Angular Misalignment

Assuming that only gravity-gradient torques are acting on the station, it is of interest to estimate the rate at which the sun-pointing axis would be misaligned if no control torques were applied. It is also relevant to evaluate the separate effects of periodic and secular gravity-gradient torques.

Since the analytical relationships do not lend themselves to a separate evaluation of the periodic component of the total torque, an exaggerated case is used to obtain an upper limit. It was thus assumed that the magnitude of the periodic component is equal to the magnitude of the total torque with $f(D)$ at the maximum value of 1.2. The periodic component acts at twice the orbital frequency and the peak value of angular misalignment was found to be 0.115 degrees during one quarter of an orbit. Hence, for the assumed numerical values, the periodic torques will not greatly influence the attitude control problem.

Angular misalignment due to the secular torques, with D_S at the maximum value of 1, was found to be

$$\Theta_{S \max} = 0.3 \text{ degrees per orbit}$$

Figure II-1 shows the accumulation of angular misalignment for the above maximum rate conditions. It is therefore seen that the accumulated error over a day would be less than 5 degrees even at the worst conditions. The superimposed oscillation due to periodic torques is also seen to be negligible by comparison.

Figure II-2 illustrates the effect of spin rate upon angular deviations. It is of interest to note the significant errors which would have been produced by the same gravity gradient torques if the vehicle were not spinning, name 13.5 degrees per quarter orbit (22.5 minutes) as compared to 0.075 degrees in the same period for a spin rate of 3 RPM. In particular, if the station were not spinning, additional control means, e.g., a momentum wheel would be required to counter the periodic torques since they would otherwise cause appreciable misalignments.

The angular stiffness of the station, illustrated by the above numerical estimates, indicates considerable latitude in the programming of control impulses. To illustrate this further, it was assumed that control impulses are applied continuously during the time when secular gravity gradient torques are near their peak value ($D_S = 1$) but that the level of the applied thrust is less than that required to completely counter the gravity gradient torque. Assuming the control thrust to be 90% of the peak gravity-gradient torque and assuming also that the latter varies sinusoidally around the peak value, it was found that the net misalignment during the time when the control torque is less than the applied torque would be 2.6 degrees. This error would be accumulated over a period of 7.8 days. This calculation is based upon a computed value for the long-term period of gravity-gradient torques of 54 days.

E. Estimates of Propellant Weight

This estimate assumes that a propellant having a specific impulse of 300 seconds is carried aboard the station to provide reaction-jet control for station orientation and orbit control. For the particular station parameters as used here, and assuming an orbital altitude of 300 n.miles, the required weight of propellant for a one year period is estimated as follows:

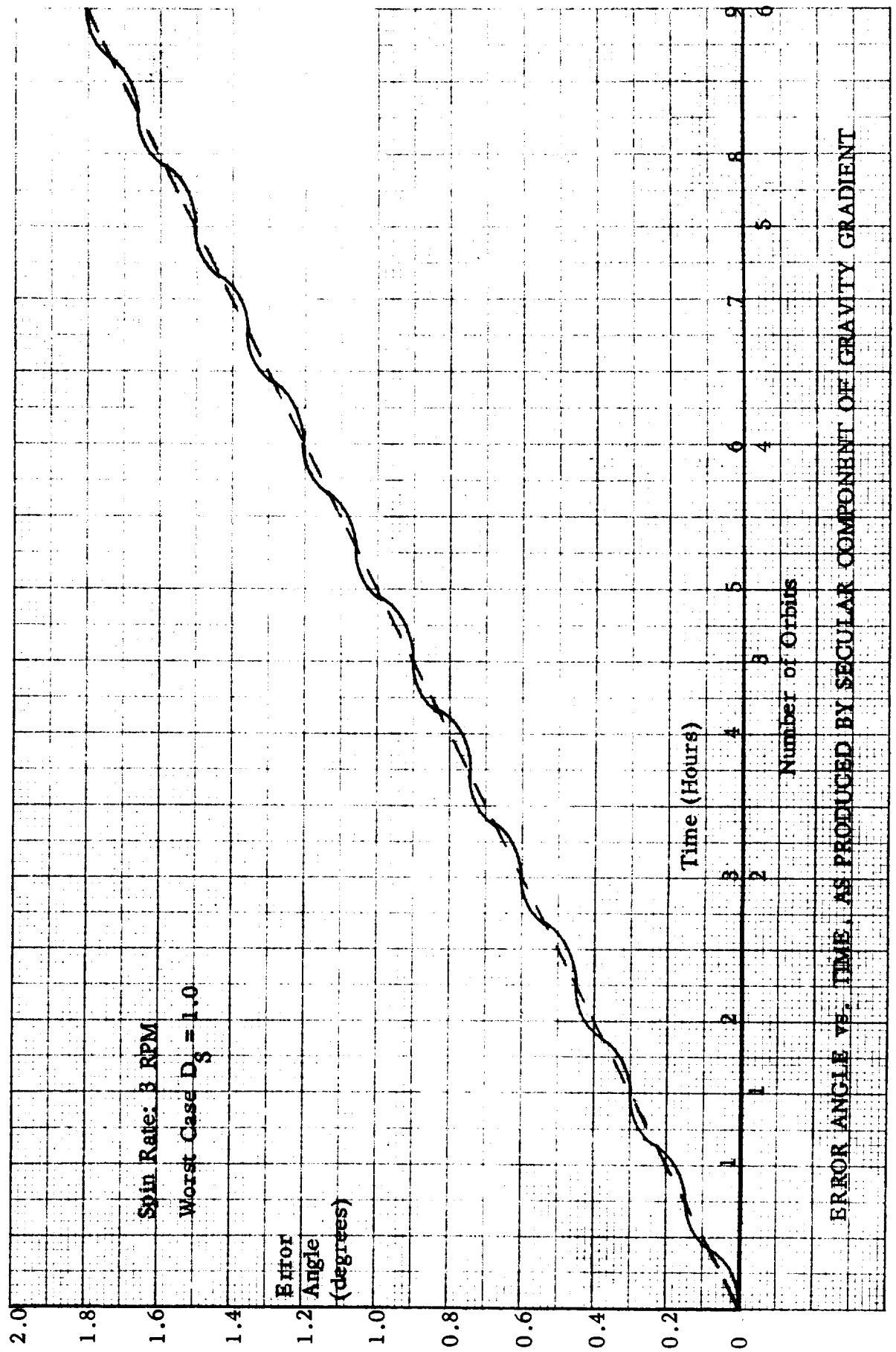
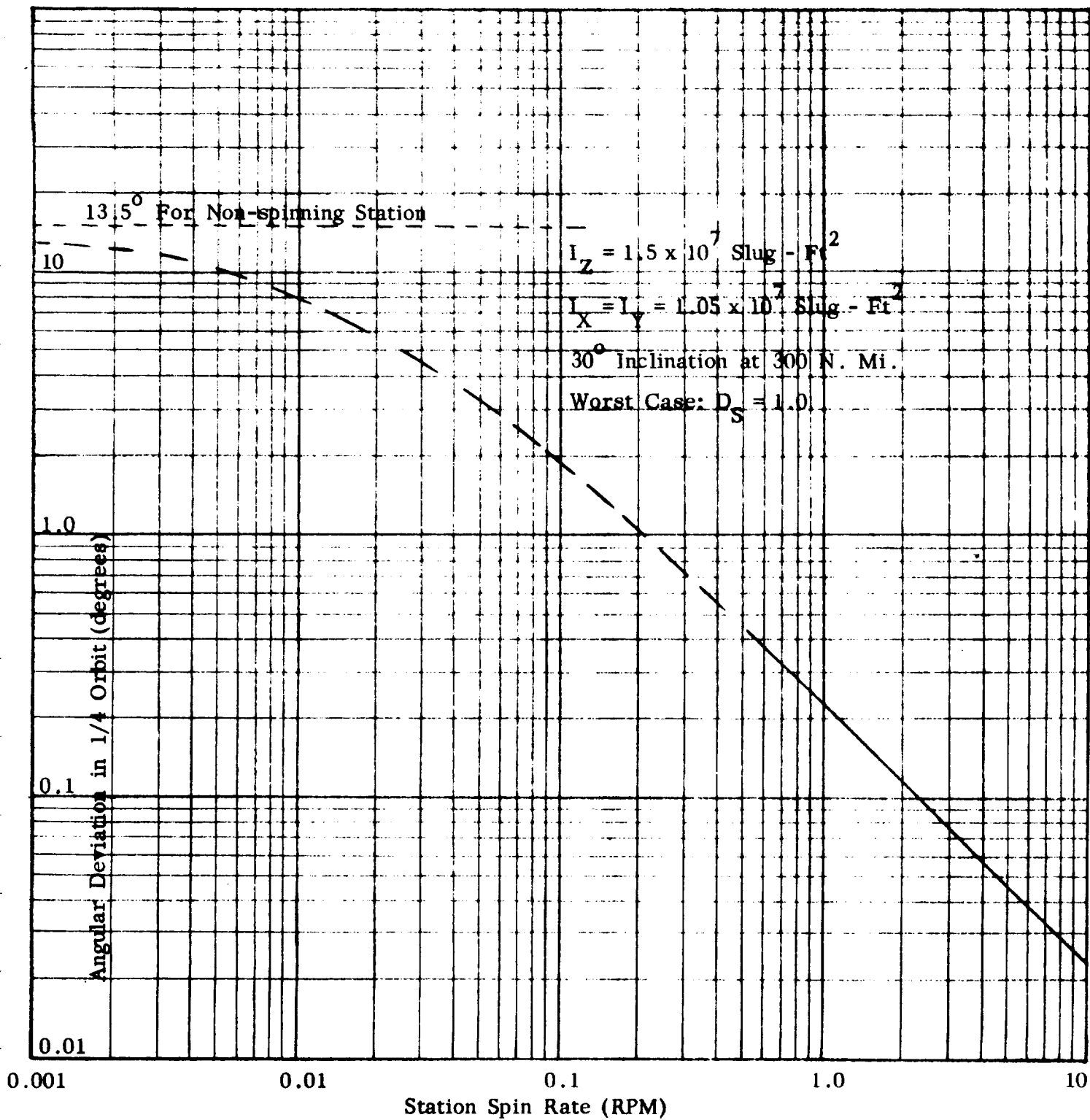


FIGURE II - 1



SUN ORIENTATION ERROR ANGLE PRODUCED BY GRAVITY GRADIENT (Secular Component)
IN ONE QUARTER ORBIT (22.5 Min.)

FIGURE II - 2

(a) It is assumed that angular orientation requirements will permit a misalignment of 0.2 degree or more. Hence, no control is provided for the periodic component of gravity-gradient torques.

(b) Angular momentum accumulation due to the secular gravity gradient torques depends upon the time variation of D_S . Since $D_S \leq 1$, an upper limit is obtained by letting $D_S = 1$. Propellant weight due to secular gravity gradient torques is thus found to be

$$W_S < 6,480 \text{ lbs per year}$$

Since D_S cannot be zero, the average value of D_S over long periods of time might be expected to be 0.6 or more. Hence

$$3,880 < W_S < 6,480 \text{ lbs/year}$$

(c) The amount of propellant to produce only the annual precession rate is calculated to be

$$W_P = 1,350 \text{ lbs per year}$$

The annual precession torque required is unidirectional and cannot, therefore, be added directly to the secular gravity-gradient torque. For, if during some portion of the year the annual precession torque adds to the gravity gradient torque, during other times it will tend to compensate for gravity gradient.

(d) The combined effect of drag causing orbit decay, and the various other disturbance torques is to require additional propellant weight comparable to that required for annual precession torque, i.e.

$$W_M \cong 1,350 \text{ lbs per year}$$

Based on the above it is estimated that chemical propellant weight for the 300 n.mile altitude would be about 6,000 lbs per year. If a chemical bipropellant rocket system were used, its total weight including propellant tankage and thrust devices would be approximately 7500 lbs for a one year life with no system redundancy.

Assuming a space station weight of 120,000 lbs, a chemical reaction control system would require about 6% of the station gross weight for a 300 nautical mile orbit. For lower altitudes, this fraction would be higher.

F. Methods of Thrust Application

The manner in which control is to be applied to a large, rotating station should be governed by the following considerations:

- (a) For a 300 n.mile altitude, about 87% of the thrust demand is predictable as regards its variation with time. This includes the requirement to correct for secular gravity gradient torques and to apply annual precession torque.
- (b) The angular stiffness of a rotating station provides a great deal of latitude in the programming of applied thrust. Thus, if an analytical prediction of thrust demand is used, it need not be extremely accurate. More significantly, however, station attitude control would not be dependent upon precise control of thrust magnitude or duration.
- (c) Station rotation can be used to permit firing of a single nozzle at the desired angular position. As previously described, this results in a reduction of propellant consumption.
- (d) Thrust requirement for orbit maintenance purposes is about 15% of the total for a 300 n.mile altitude. Since a single nozzle does not produce a pure couple on the station, it is possible to program the attitude control impulses from a single thrust device so that when the station is moving away from the sun, the impulses occur with a different frequency from when it is moving towards the sun. This will produce a net force on the station, opposing the drag force which causes orbit decay. If two-thrust devices are used, one on the sunward side and one on the shadow side, the air drag compensation can be accomplished even more efficiently as a byproduct of attitude control impulses.

Since the angular position (in the plane of the station) at which thrust is applied is one of the control parameters, thrust duration must be sufficiently short so as not to spread it over too large an angle by virtue of station rotation. Otherwise the effective moment arm of the impulse would be reduced. Figure II-3 shows the efficiency of thrust application as a function of the ratio of firing time to the period of station rotation. For the assumed rate of 3 RPM and for a firing time of 2 sec the efficiency is seen to be about 92%.

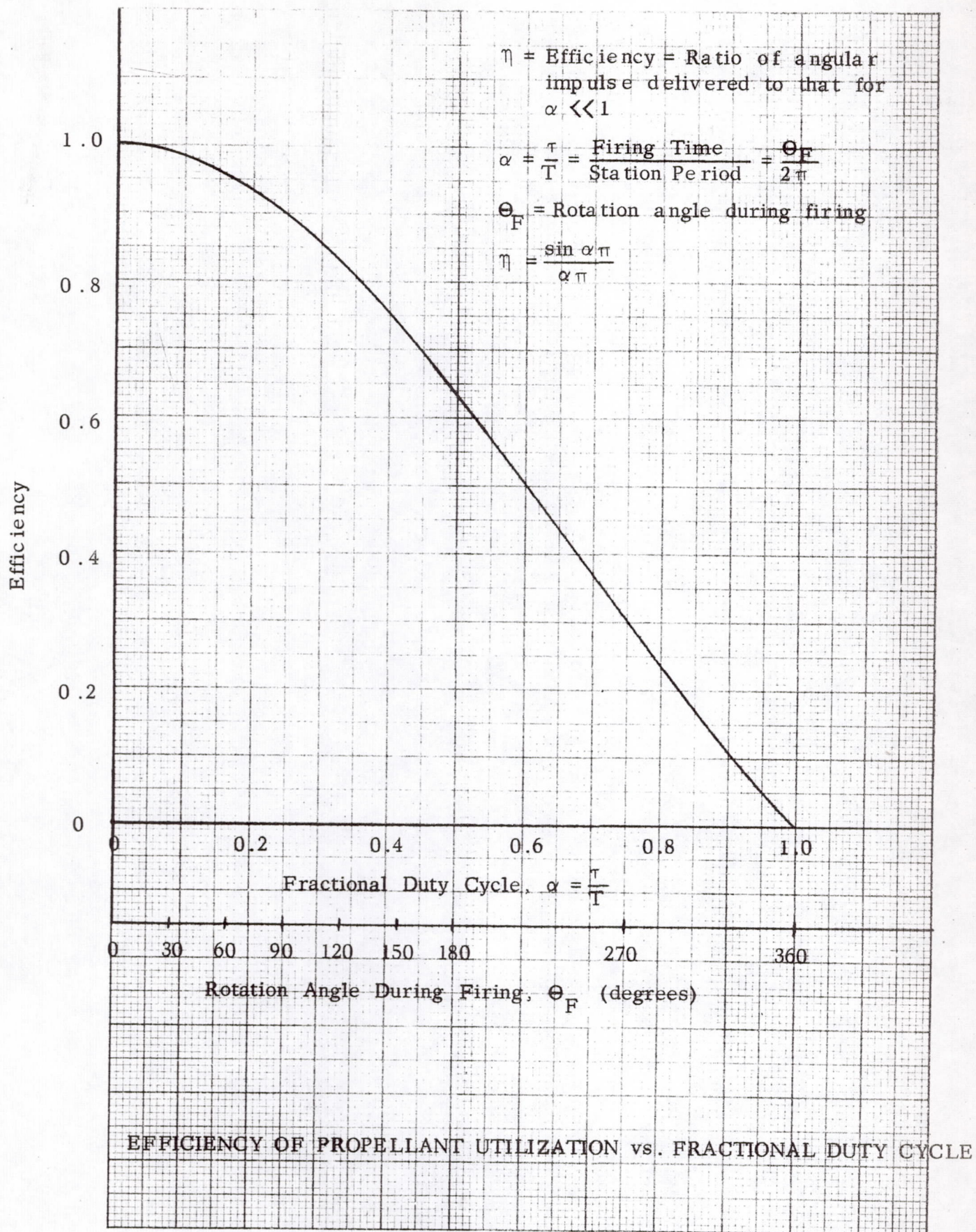


FIGURE II - 3

III DESIGN STUDIES OF AN ELECTRICALLY-HEATED PULSE ROCKET (OHMJET) THRUST SYSTEM

A. General Discussion -

The inherent advantage of using waste carbon dioxide from a manned space station as the propellant for attitude control can only be realized through an efficient means of recovery and utilization of this waste product. It is assumed that a molecular sieve bed is used to absorb CO_2 . Two basic methods for recovery of CO_2 are described and analyzed in this section; they are:

Method I: Removing the carbon dioxide from the molecular sieve bed by heating the bed until the CO_2 partial pressure is raised to 14.7 psia; compressing this gas to ten atmospheres and storing it in a storage bottle, then exhausting it periodically, as required, through a small Ohmjet.

Method II: Removing the carbon dioxide from the molecular sieve bed as above, but instead of compressing and storing the CO_2 , exhausting it as required directly through an Ohmjet which is designed to operate with an inlet pressure of one atmosphere.

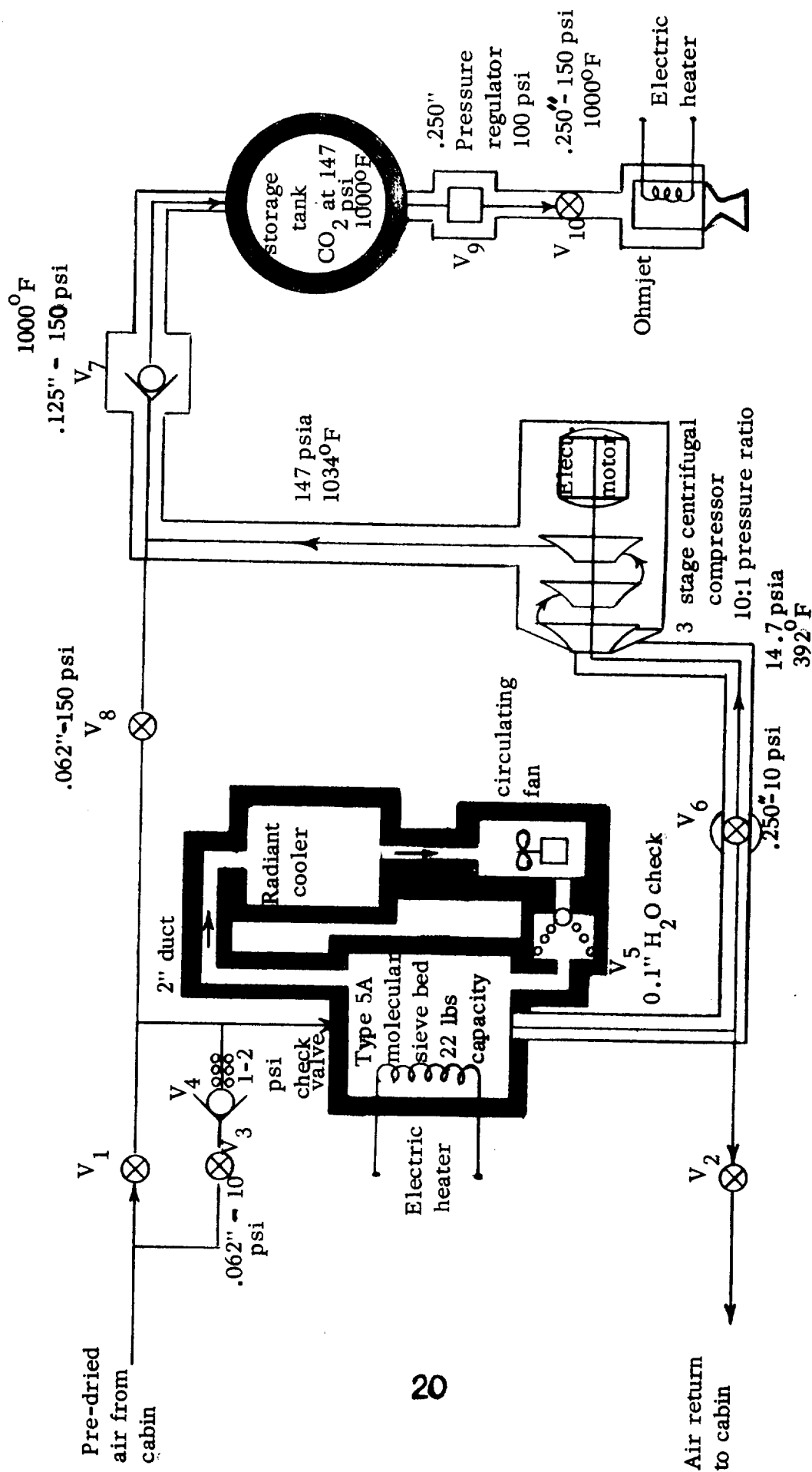
Systems were sized for both these methods and the component weights, peak power, and average power requirements were estimated for two recovery duty cycles.

For all design studies in this section it is assumed that the space station has two identical Ohmjet systems, each operating on a 90 minute cycle with the cycles staggered in time by 45 minutes. Therefore, one system is applying thrust impulses for 45 minutes while the other system is absorbing CO_2 .

B. Description of Carbon Dioxide Recovery Systems -

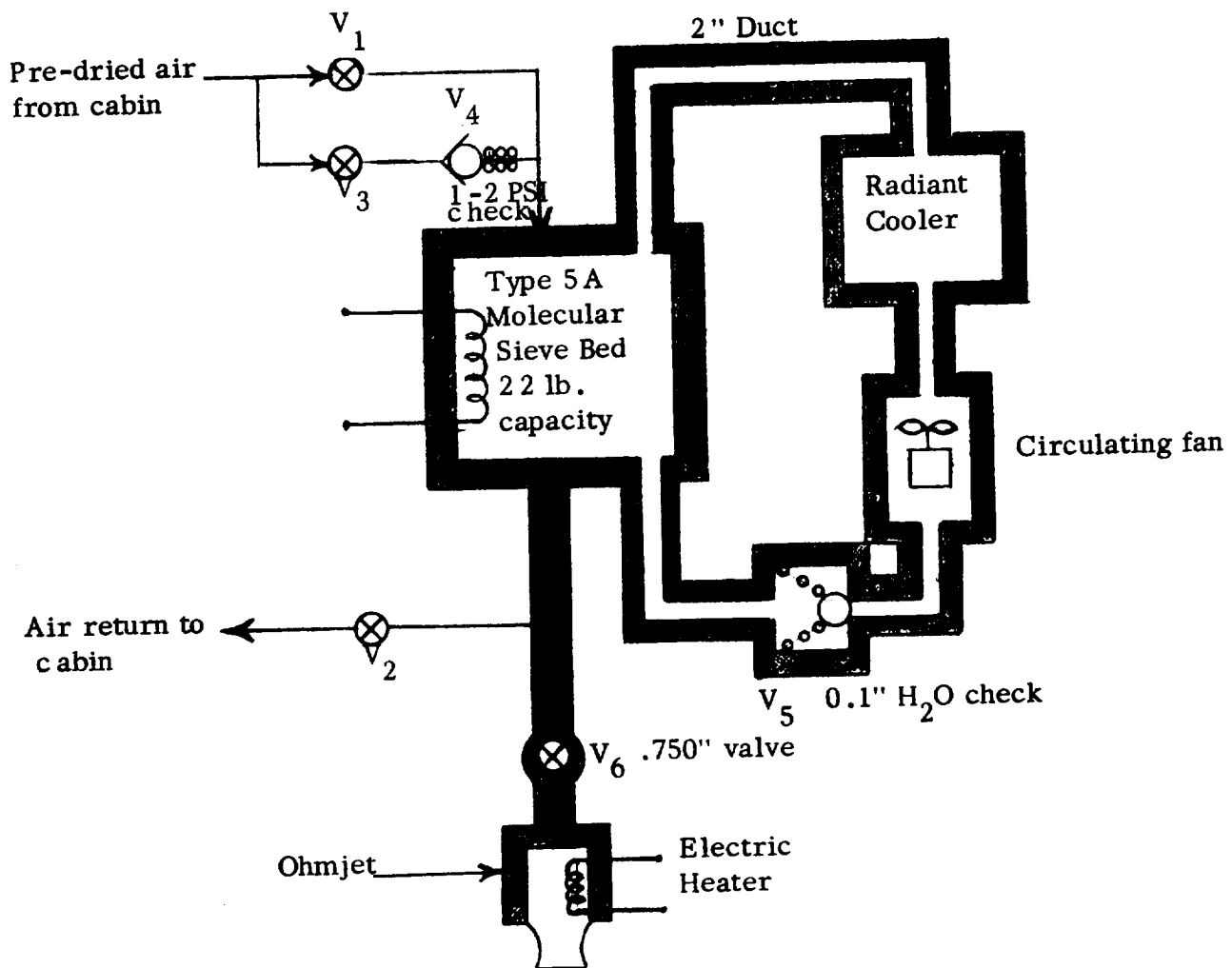
(1) General:

The schematics of the two methods of CO_2 recovery systems are shown in Figures III-1 and III-2. Continuous operation of a pair of these systems, located at diametrically opposite positions on the station is required for proper attitude control and orbit maintenance. During the first half of an orbit, one system (system A) is adsorbing CO_2 from the cabin air, while the second system (system B) is going through its regeneration and recovery cycle. During the second half of the orbit, system B is adsorbing CO_2 while the sieve bed of system A is being regenerated and CO_2 recovered. Compensation for aerodynamic drag on the space station is achieved if the Ohmjet of System A is directed to



SCHEMATIC DIAGRAM OF CO₂ RECOVERY, PRESSURIZATION AND STORAGE SYSTEM,
METHOD I

FIGURE III - 1



SCHEMATIC DIAGRAM OF CO₂ RECOVERY SYSTEM FOR DIRECT USE OF CO₂ FROM MOLECULAR SIEVE BED, METHOD II

FIGURE III - 2

apply thrust toward the sun while the station is on the half-orbit approaching the sun, and the Ohmjet of System B applies thrust away from the sun while the station moves away from the sun, as shown schematically in Figure III-3.

(2) Molecular Sieve Bed:

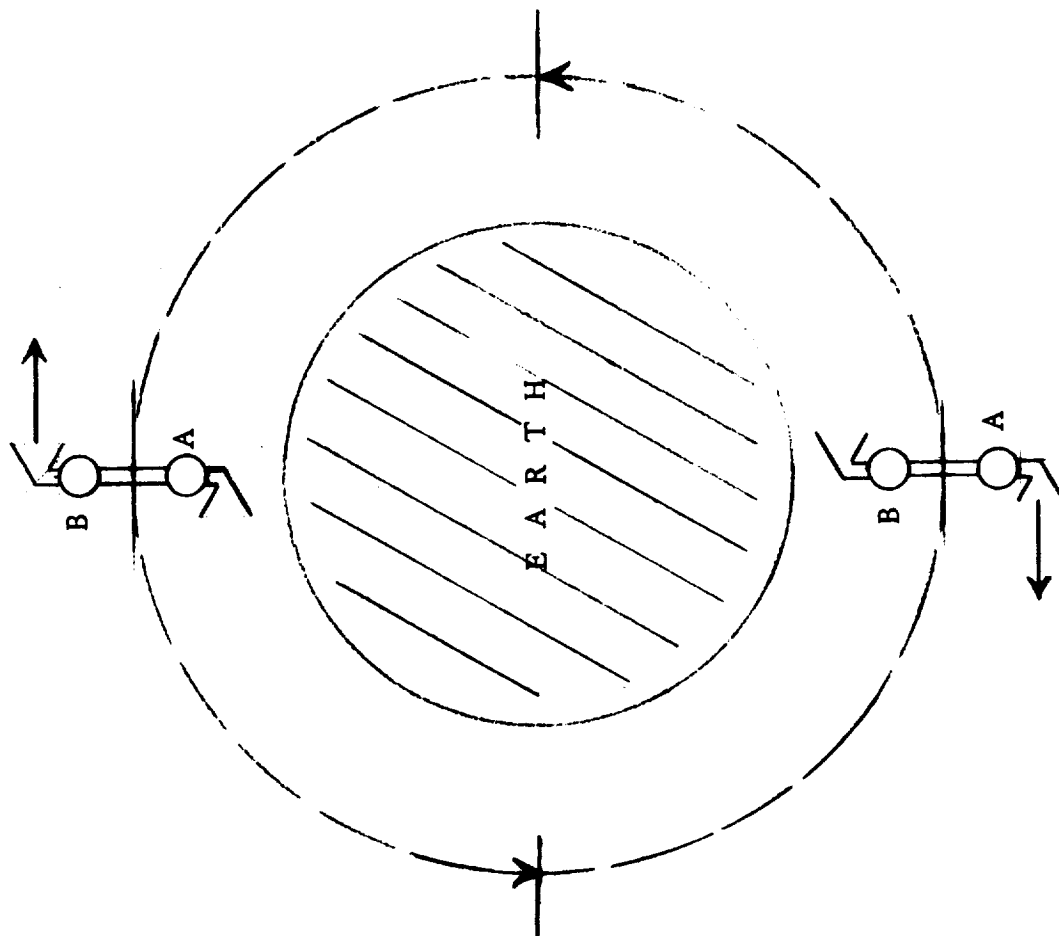
As can be seen from Figures III-1 and III-2, the molecular sieve bed and its electrical heater for regeneration are identical for both methods. The size and operation of this system will be discussed in detail in this section.

The adsorbent material used in the CO₂ removal bed is Linde Type 5A molecular sieve material. During the adsorption cycle, all valves of the system are closed except V₁ and V₂ and predried cabin air is passed through the pelletized bed material, the temperature of which is approximately 77° during this phase of the cycle. At this temperature the molecular sieve bed material (See Figure III-4) will hold 0.08 pounds of CO₂ per pound of adsorbent at a CO₂ partial pressure of 8 mm of mercury (the maximum permissible in the cabin air). Since it is required to recover the CO₂ adsorbed by the bed, the normal method of regenerating the molecular sieve material by venting to space vacuum cannot be used. Instead it is proposed to heat the bed electrically to 392° F. during which time all valves would be closed. At this temperature the partial pressure of the CO₂ is increased to one atmosphere absolute. Carbon dioxide can then be drawn from the bed at 760 mm of mercury. (This gas would be piped to the compressor inlet in Method I and directly to the Ohmjet in Method II.) The molecular sieve bed material at this temperature (392° F.) and pressure (760 mm of Hg) will hold 0.023 lbs. of CO₂ per pound of adsorbent. Each regeneration cycle could therefore remove 0.08-0.023 = 0.057 lbs. of CO₂ per pound of adsorbent.

The energy required to heat each pound of the bed material for regeneration is $C_B \Delta T$ where C_B is the specific heat of the bed material and ΔT is the temperature rise. If we assume $C_B = 0.2$ BTU/lb. - °F and set $\Delta T = (392^\circ \text{ F.} - 77^\circ \text{ F.}) = 315^\circ \text{ F.}$, then the energy required to heat the bed for regeneration is $Q = 63$ BTU/lb. or 18.4 watt hours/lb.

Upon completion of regeneration it is necessary to cool the molecular sieve bed down to its original temperature of 77° F. before the adsorption can begin. This means that the 63 BTU per pound of bed material must be removed. For this cooling cycle all valves except V₃ are closed. The circulatory fan is started, opening check valve V₅. The fan circulates the gas in this closed system through the bed to a radiant cooler and

System B fires during this portion
of orbit



Thrust from thrusters which is used to
compensate gravity gradient torques
also supplies impulses to overcome
aerodynamic drag

SCHEMATIC DIAGRAM SHOWING THRUST CYCLE
TO ACCOMPLISH ORBIT MAINTENANCE

Figure III - 3

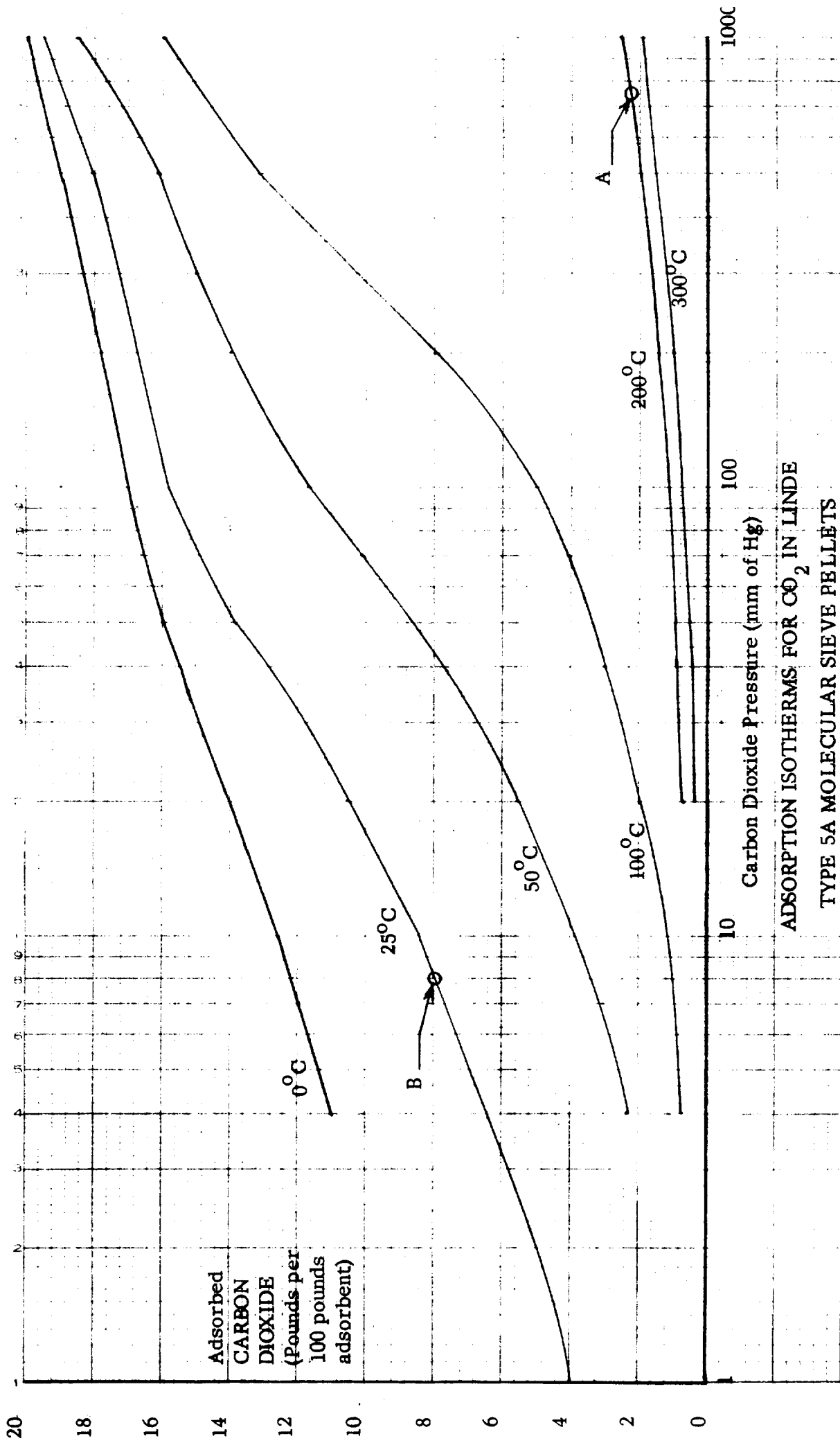


FIGURE III - 4

thence back through the bed. Heat is removed from the circulating gas by the cooler and radiated to space. As the bed cools, the pressure in this closed loop drops. To prevent this pressure from dropping too low and decreasing the heat transfer capacity of the system, a small quantity of cabin air is sucked into the system through Valve V_3 and check Valve V_4 to maintain the pressure near cabin ambient. When the bed temperature is again reduced to 77° F. the bed is ready to start another adsorption cycle.

(3) Method I: Compressor, Storage Tank and Ohmjet:

When the molecular sieve bed reaches the regeneration temperature of 392° F. Valve V_6 is opened and the centrifugal compressor is started. Carbon dioxide is driven from the bed and enters the compressor at one atmosphere and 392° F. It is compressed and is discharged from the compressor at 10 atmospheres and about 1000° F. through check Valve V_7 into the storage tank. In order to purge the bed properly, a small quantity of CO_2 is bled through Valve V_8 and recirculated through the bed. The storage tank has the capacity to store the amount of CO_2 recovered during one cycle. This storage tank acts as an accumulator which assures that CO_2 at 6 to 7 atmospheres is available to the Ohmjet which is operated for 2 seconds out of every 20 seconds during the regeneration cycle of 4.5 to 8.0 minutes each half-orbit. The complete system including the molecular sieve bed must be well insulated to minimize heat losses. Because the inlet pressure is between 6 and 7 atmospheres the size of the Ohmjet for Method I is relatively small. Also the heating element need only raise the gas temperature from 1000° F. to 1600° F., which is the desired nozzle inlet temperature.

(4) Method II: Direct Ohmjet, Operating at One Atmosphere Pressure:

In this method, the compressor and storage tank are eliminated and the gas is supplied at one atmosphere and 392° F. directly to the Ohmjet through Valve V_6 . In this method, there is no need for an accumulator, because the gas volume in the molecular sieve bed and piping is sufficient to maintain relatively constant pressure to the Ohmjet during its two seconds of operation every twenty seconds for 4.5 to 8.0 minutes each half-orbit. This complete system is also well insulated to minimize heat losses. With this method, the inlet pressure is low (one atmosphere), the Ohmjet is relatively larger and the heating element must be capable of raising the gas temperature from 392° to 1600° F. The inlet valve to the Ohmjet, however, operates at only 392° F. instead of at 1000° F. as in Method I and should therefore be more reliable.

C. Sizing of System Components -

(1) Basic Assumptions: The sizing of each component for both methods is based on the following assumptions:

- (a) There are 21 men on the space station.
- (b) Each man generates an average of 1.88 lb. of CO_2 per day.
- (c) A maximum of 300 lb.-sec. impulse per orbit is required from the Ohmjets to control attitude and maintain orbit altitude of the station.
- (d) Station rotates at 3 rpm.
- (e) Ohmjet electrical efficiency is 90 per cent.
- (f) Nozzle thrust coefficient of Ohmjet is 1.7.
- (g) Specific impulse of CO_2 is 60 sec. at 520°R . and varies as the square root of nozzle inlet temperature .
- (h) Cooling motor-fan is 50 per cent efficient.
- (i) Compressor has an efficiency of 70 per cent.
- (j) Compressor motor efficiency is 75 per cent.
- (k) Each kilowatt of power (average) requires 350 lbs. of auxiliary power equipment (e.g. solar cells and batteries).

(2) Duty Cycles:

The size and power requirements of each method depends directly on the duty cycle of the recovery system. In order to show the general effect of duty cycle on these basic parameters, the size, weight and power requirements of the components are derived for the following two cycles, based on a 90 minute orbital period (only cycle 2 has a longer bed heat up time and regeneration time to reduce peak electrical power demand):

System A	System B	Duty Cycle 1	Duty Cycle 2
Adsorb	Heat Bed	0 to 4.5 min.	0 to 8 min.
↓	Regenerate and Pulse	4.5 to 9.0 min.	8 to 16 min.
	Cool Bed	9.0 to 45.0 min.	16 to 45 min.
Heat Bed	Adsorb	45 to 49.5 min.	45 to 53 min.
Regenerate and Pulse	↓	49.5 to 54.0 min.	53 to 61 min.
Cool Bed		54 to 90 min.	61 to 90 min.

(3) Molecular Sieve and CO₂ Recovery System:

(a) Adsorbent Required. The CO₂ bed of each system must absorb all the CO₂ generated by the 21 man crew during half an orbit (45 minutes). If we assume the average rate of CO₂ generation per man is 1.88 lb./day, the total CO₂ to be adsorbed is 39 lb./day. During the adsorption cycle, each bed must therefore remove 1.24 lb. per cycle. As calculated previously, each pound of adsorbent can remove 0.057 lb. of CO₂ per cycle. The required weight of adsorbent per bed is then 21.8 pounds.

(b) Electrical Heating Requirements. The energy required to heat each pound of adsorbent from 77° to 392° F. was previously calculated to be 18.4 watt hours. The total energy to heat the required 21.8 lb. of adsorbent material is then 400 watt hours. This energy must be supplied during the bed heating cycle. The power level required to heat the bed is then 3000 watts for Duty Cycle 2. In addition it is assumed that 400 watts is required to maintain the bed at temperature during the regeneration cycle.

(c) Cooling system. If we neglect the heat loss from the bed through the insulation, the amount of energy added to the bed during heating (400 watt-hrs.) must be removed from the bed during the cooling cycle to return the bed temperature from 392° F. to 77° F. The cooling system for the molecular sieve bed consists of a radiator and circulating fan in series with the molecular sieve bed.

We define: w_g = circulation gas flow rate
 T_{in} = gas inlet temperature to radiator
 T_{out} = gas outlet temperature from radiator
 T_B = average temperature of bed
 T_R = average temperature of radiator
 Q_R = radiation heat transfer rate
 A_R = radiator area

If we assume $T_{in} = T_B$
$$T_R = \frac{T_{in} + T_{out}}{2}$$

and
$$Q_R = \epsilon \sigma A_R T_R^4$$

where σ = Stefan Boltzman constant
 ϵ = radiator surface emissivity (0.8)

$$\text{then } w_g C_p (T_{in} - T_{out}) = \epsilon \sigma \left(\frac{T_{in} + T_{out}}{2} \right)^4 A_R$$

$$\text{and } w_g C_p (T_{in} - T_{out}) = W_B C_B \frac{dT_{in}}{dt}$$

$$\text{where } C_p = 0.205 \text{ BTU/lb.}^\circ\text{R for CO}_2$$

$$C_B = 0.20 \text{ BTU/lb.}^\circ\text{R for sieve bed}$$

$$W_B = 21.8 \text{ lb.}$$

From the above two equations, the molecular sieve temperature as a function of time is calculated and presented graphically in Figure III-5 for two circulation rates and two radiator areas.

The temperature histories show in Figure III-5 do not account for any additional heat losses through the bed, piping or radiator internal wall, which would increase the rate of cooling. With this in mind, it is judged that a 10 square foot radiator with a 1.17 lb./min. (~ 10 CFM) circulatory fan would be sufficient for the 36 minute cooling cycle of Duty Cycle 1 and that a 12 square foot radiator with a 1.75 lb./min. (~ 15 CFM) circulating fan would be adequate for the 29 minute cooling cycle of Duty Cycle 2.

The radiator is assumed to be a plate of 0.0625" aluminum with internal cooling channels. The inner surface is covered by one inch of insulation to minimize heat transfer into the cabin.

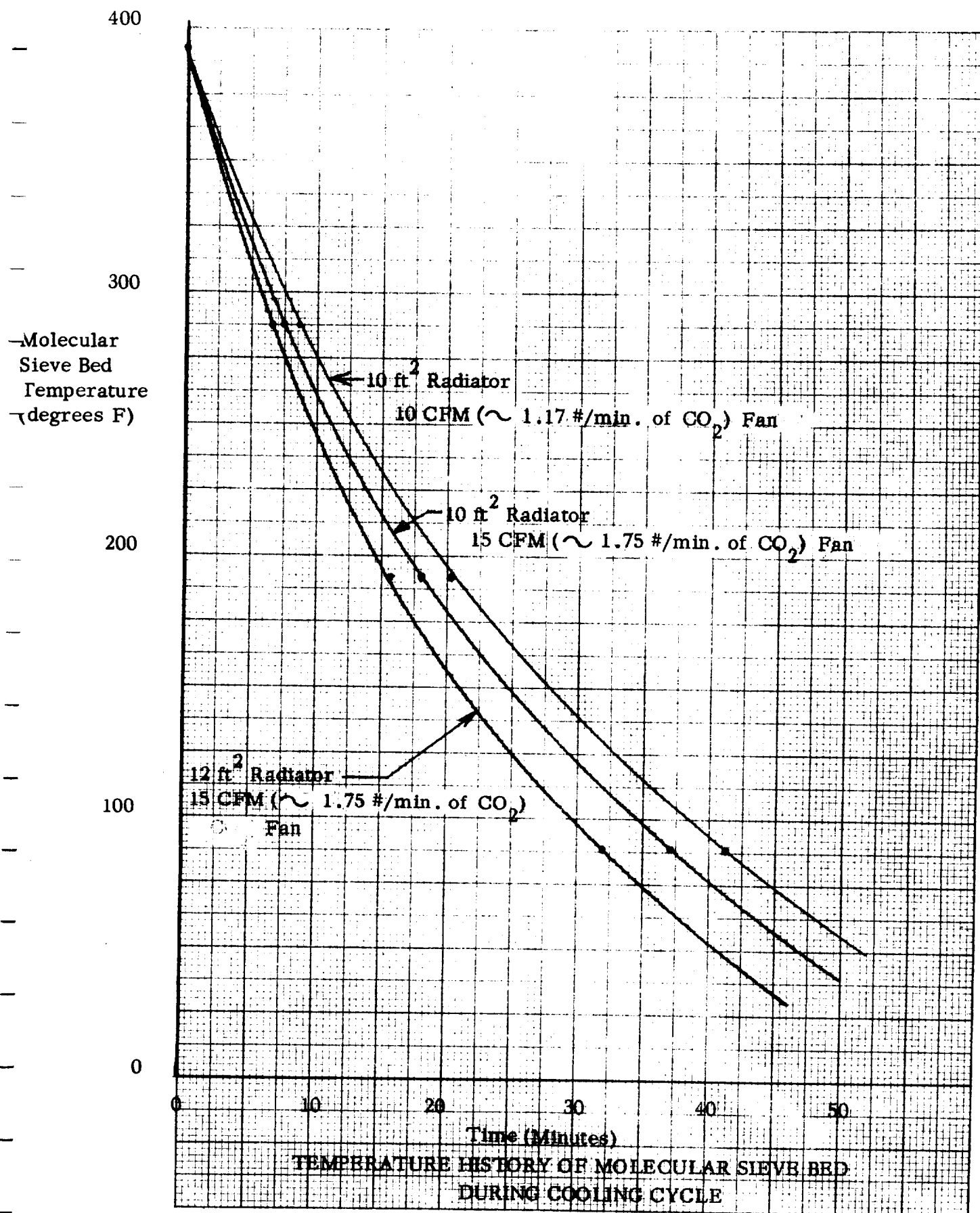


FIGURE III - 5

It is estimated that the radiator would weigh 1.69 lb./ft.², consisting of 1.44 lb. of aluminum and 0.25 lb. of insulation. Duty Cycle 1 requires a 10 ft.² of radiator which would weigh 16.9 lbs. and Duty Cycle 2 requires a 12 ft.² radiator which would weigh 20.3 lbs.

The flow rates of the circulating fan have been established and an estimate of the head against which it must operate is required to establish its power requirements. Conservative estimates of the head requirements are tabulated below for 10 CFM and 15 CFM flow rates:

ITEM	10 CFM	15 CFM
Velocity head for 2" i.d. pipe	0.021 in of H ₂ O	0.046 in of H ₂ O
Check valve pressure loss	0.100 in of H ₂ O	0.100 in of H ₂ O
Radiator pressure loss	1.400 in of H ₂ O	2.200 in of H ₂ O
Pipe Friction	0.063 in of H ₂ O	0.142 in of H ₂ O
Bed loss	1.400 in of H ₂ O	3.150 in of H ₂ O
TOTAL HEAD	2.984 in H ₂ O	5.638 in H ₂ O
Air Power	155 ft. lb./min.	4.38 ft. lb./min.
Efficiency of fan	50 %	50%
Efficiency of motor	70%	70%
Power requirement of motor	443 ft. lb./min. or 10 watts	1250 ft. lb./min. or 28.3 watts

(d) Compressor -

The compressor in Method I must pump the 1.24 lb. of CO₂ generated from 1 to 10 atmospheres during the regeneration cycle. The work required to compress this gas isentropically is expressed by

$$\Delta h_s = \frac{RT_1}{k-1} \left[1 - \left(\frac{P_2}{P_1} \right)^{\frac{k-1}{k}} \right]$$

where Δh_s = work per unit weight of gas

R = gas constant

T₁ = inlet temperature

k = ratio of specific heats

P₁ = inlet pressure

P₂ = discharge pressure

Substituting the values $R = 35.1 \text{ ft.}^{\circ}\text{R.}$, $T_1 = 852^{\circ}\text{R.}$, $P_2/P_1 = 10$, and $k = 1.28$ in the above expression we get $\Delta h_s = 70,000 \text{ ft.}$ The energy required to isentropically compress the CO_2 is therefore $86,900 \text{ ft. lb./cycle}$. Assuming adiabatic compression with a compressor of efficiency of 70 per cent, temperature rise in the compressor would be 950°F. The compressor discharge temperature would be 1800°R. or 1340°F. Allowing for heat conduction into the compressor during the short period of compressor operation, it is probable that the gas exit temperature would be reduced to an actual value near 1000°F.

The power to drive the compressor should be supplied at a high speed (24,000 rpm motor). If this motor has 75 per cent efficiency, the input power P_m , required by this motor is 840 watts for Duty Cycle 1 and 470 watts for Duty Cycle 2. Motors of this size operating at 24,000 RPM weigh about 2-1/2 to 3 lbs. per kilowatt. Therefore, the motor weight is estimated at 2.2 lbs. for Duty Cycle 1 and 1.4 lbs. for Duty Cycle 2.

A high speed 2 or 3 stage compressor for such an application would have a diameter of about 10" and width of 1.5" with a metal solidity of about 1/3. Its weight therefore is estimated as:

$$\frac{\pi}{4} (10)^2 \times 1.5 \times 1/3 \times 0.286 = 11.2 \text{ lbs.}$$

There would be little difference in weight in the compressor required for either Duty Cycle.

(e) Storage Tank. The storage tank is designed to hold the complete amount of CO_2 regenerated in one cycle at a temperature of 1500°R. and a pressure of 147 psia. The tank volume is calculated to be 3 ft.^3 . The lightest structure which will hold this volume is a spherical tank with an internal diameter of 1.79 ft. The required wall thickness is calculated to be 0.020 in. for a working stress of 40,000 psi in stainless steel. The pressure shell of the tank would weigh 8.3 lbs.

To minimize heat loss from the stored gas, the tank is covered by 2" of insulation covered with an external cover of 0.010" thick aluminum. The weights of these two items are 6 lbs. and 2 lbs. respectively making the total weight of the storage tank 16.3 lbs.

(f) Ohmjets. During each orbit, 2.48 lbs. of CO_2 are exhausted through the Ohmjets. In order to obtain the total 300 lb-sec/orbit impulse required, the specific impulse of the CO_2 must be 121 seconds. For CO_2 this value of specific impulse corresponds to a gas temperature of approximately 1600°F.

During the regeneration cycle, the Ohmjet is given a 2 second pulse once every 20 seconds (once each revolution of the station). The heating element of the Ohmjet is operated

for 1-1/2 seconds preceding and during the 2 second pulse of gas flow for a total of 3-1/2 seconds each 20 seconds.

For Method I, the total energy put into the gas by the Ohmjet is 90 watt hours/orbit. If we assume an Ohmjet efficiency of 90 per cent, the energy supplied to the Ohmjet is 100 watt hours/orbit.

For Duty Cycle 1, there are 27 pulses per orbit, therefore each pulse must consume 3.71 watt hours in 3-1/2 seconds. The power required by the Ohmjet is therefore 3810 watts. For Duty Cycle 2, there are 48 pulses per orbit, thus the power required by the Ohmjet is 2140 watts.

A total impulse of 300 lb. -sec. /orbit is assumed to be required from the Ohmjets. This impulse equals the product of the thrust, F , and the time of operation per orbit. The Ohmjet thrust is also expressed by

$$F = P_1 A_t C_F$$

where P_1 = the Ohmjet nozzle inlet pressure

A_t = the Ohmjet nozzle throat area

C_F = the nozzle thrust coefficient

Assuming $P_1 = 100$ psia, and $C_F = 1.7$:

$$A_t = \frac{F}{170} \text{ square inches}$$

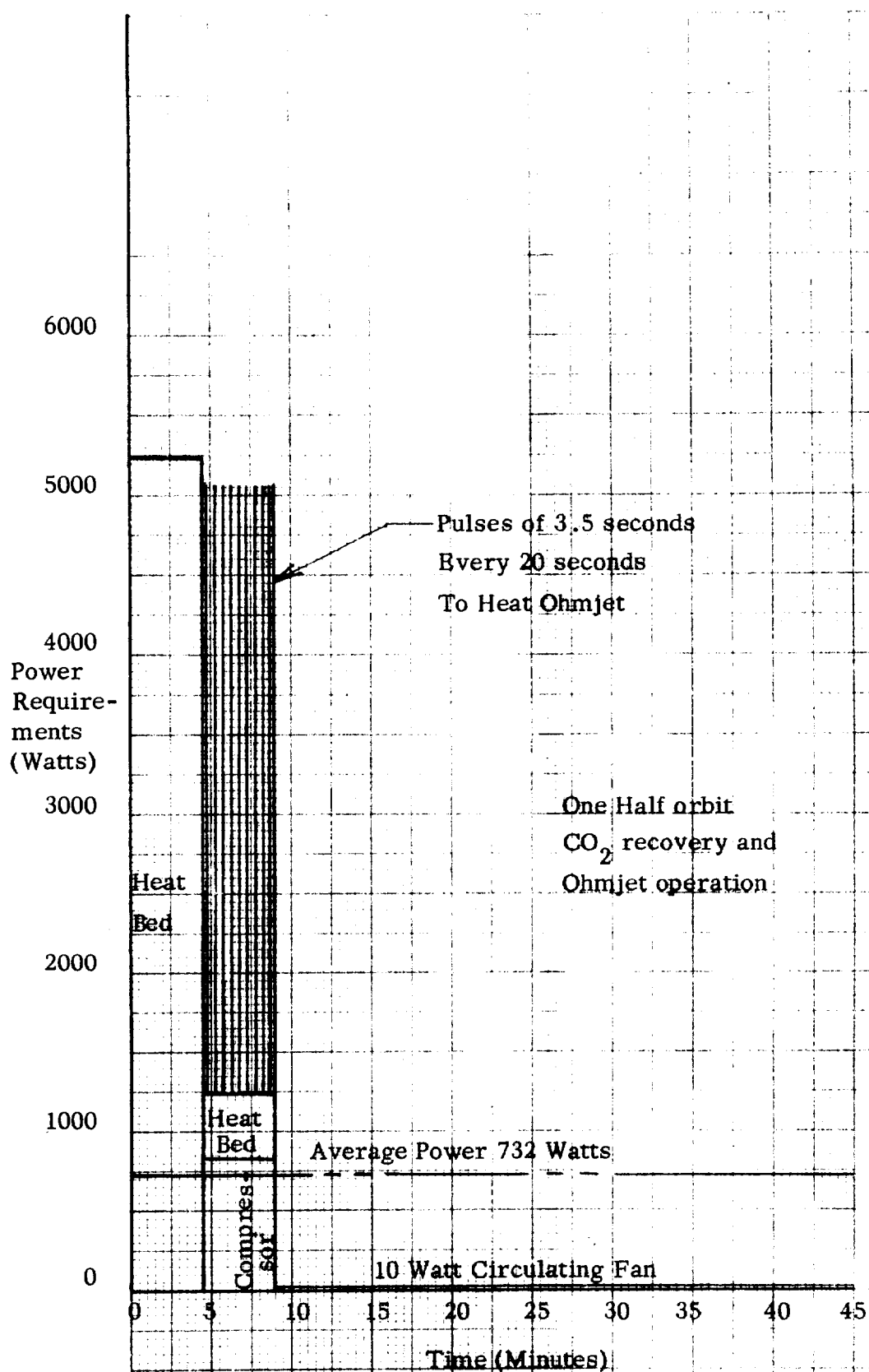
For Duty Cycle 1, the Ohmjet thrust is 5.56 lbs., which requires a nozzle throat area of 0.0328 in² (0.204 in diameter).

For Duty Cycle 2, the Ohmjet thrust is 3.13 lbs., which requires a nozzle throat area of 0.0184 in² (0.153 in diameter).

Using the same procedure as above, the Ohmjet energy requirements for Method II are calculated to be 201 watt hours/orbit. The power level required by the Ohmjet is 7690 watts for Duty Cycle 1 and 4310 watts for Duty Cycle 2. For Duty Cycle 1, the required Ohmjet thrust of 5.56 lbs. requires a nozzle throat area of 0.223 in² (0.532 in diameter) and for Duty Cycle 2, the Ohmjet thrust of 3.13 lbs. requires a nozzle throat area of 0.125 in² (0.400 in diameter).

D. Electrical Power Requirements -

The power requirements for each method and both duty cycles are summarized in Table I and shown graphically as a function of time in Figures III-6, 7, 8, and 9.



POWER REQUIREMENTS, METHOD I, DUTY CYCLE 1

FIGURE III- 6

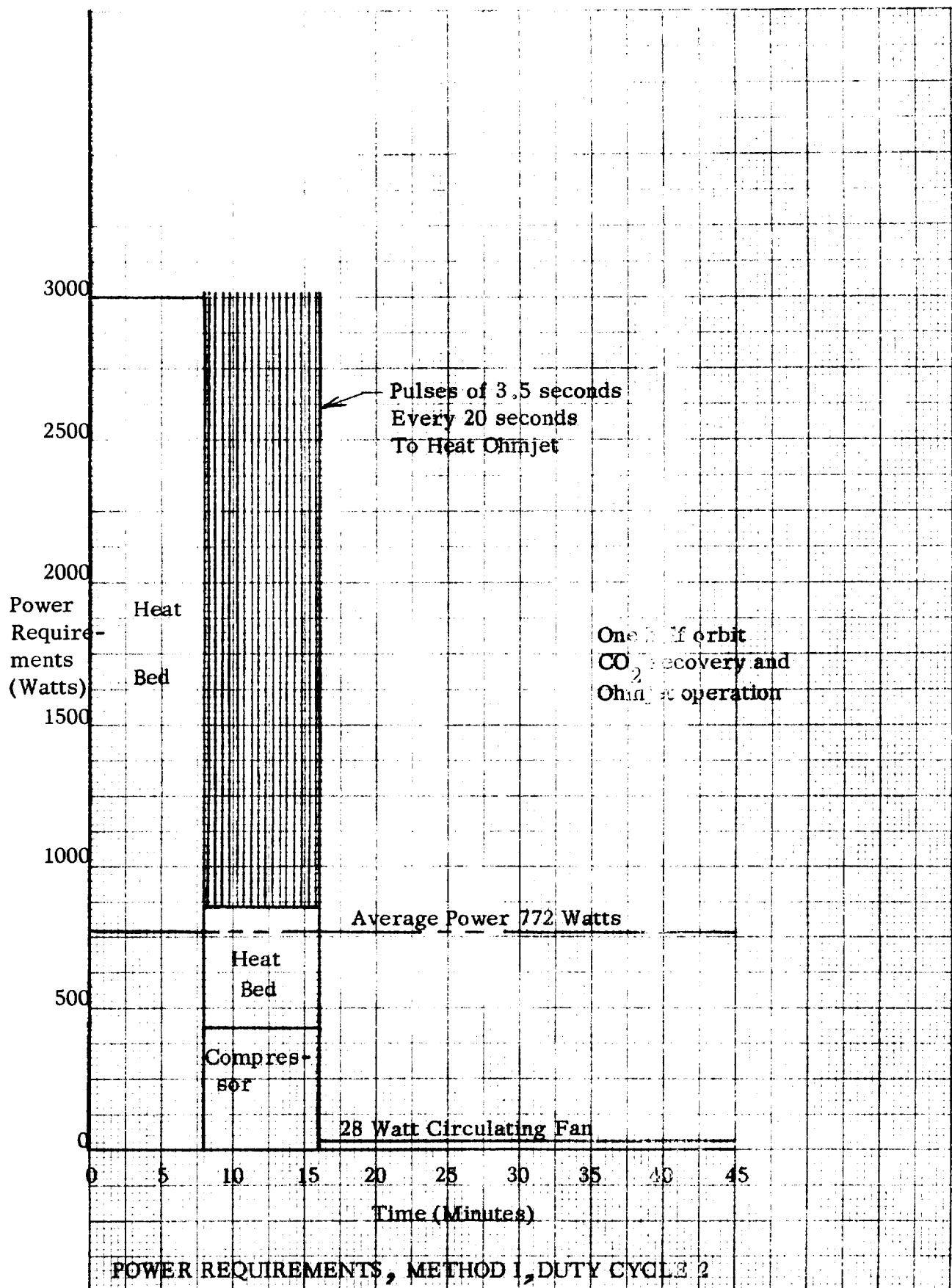


FIGURE III - 7

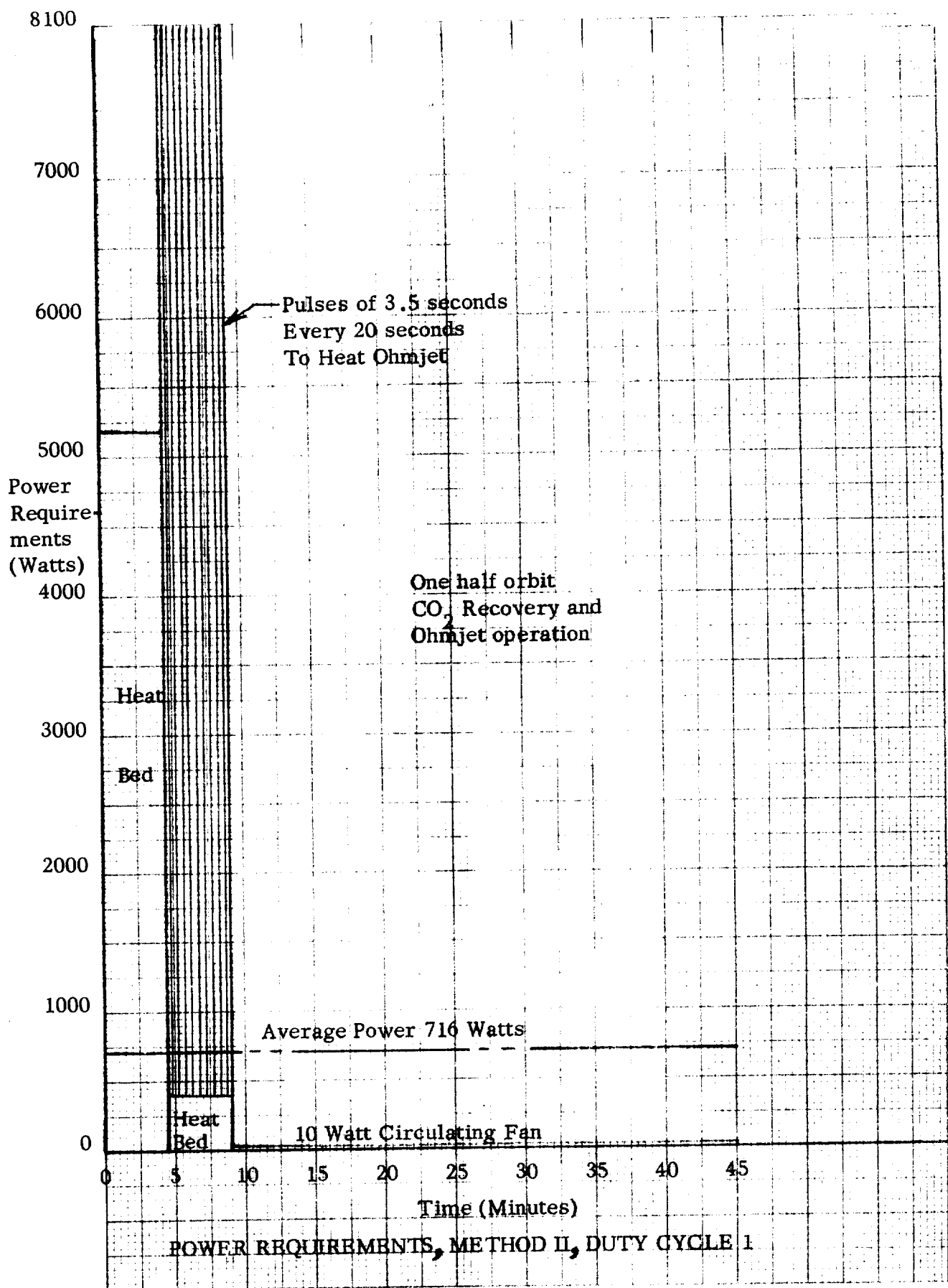


FIGURE III- 8

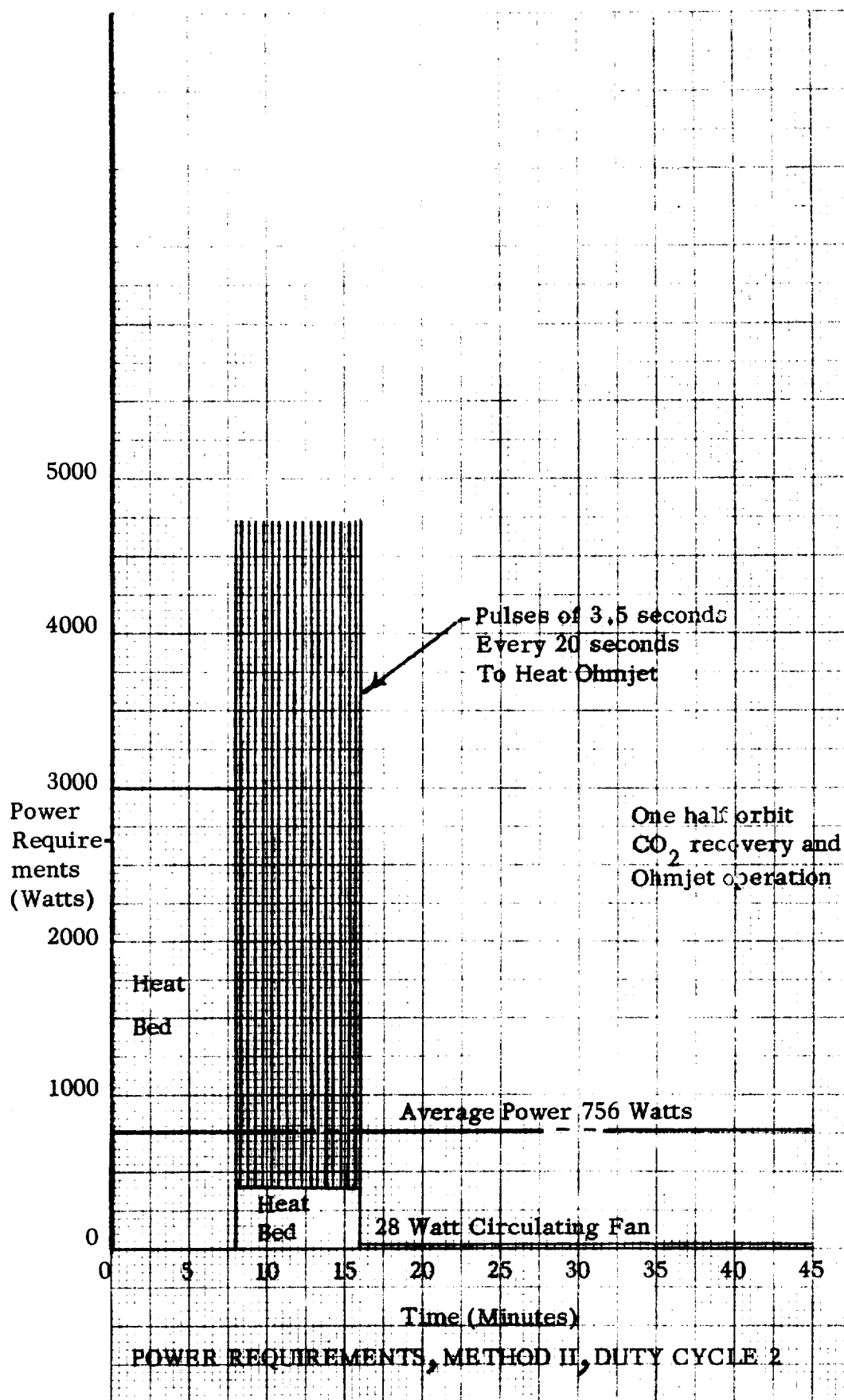


FIGURE III- 9

TABLE III - 1

ELECTRICAL POWER REQUIREMENTS FOR OHMJET FOR TWO DUTY CYCLES

DUTY CYCLE 1

TIME	FUNCTION	METHOD I		METHOD II	
		Peak Power (watts)	Total Energy (watt-hours)	Peak Power (watts)	Total Energy (watt-hours)
0 to 4.5 min	Heat bed B	5330	400	5330	400
4.5 to 9 min	Regenerate and Pulse	5050	143	8090	131
9 to 45	Cool bed B	10	6	10	6
45 to 49-1/2	Heat bed A	5330	400	5330	400
49-1/2 to 54	Regenerate and Pulse	5050	143	8090	131
54 to 90	Cool bed A	10	6	10	6
1 orbit	TOTAL	5300	1098	8090	1074
		Average Power = 732 watts		Average Power = 716 watts	

DUTY CYCLE 2

TIME	FUNCTION	METHOD I		METHOD II	
		Peak Power (watts)	Total Energy (watt-hours)	Peak Power (watts)	Total Energy (watt-hours)
0 to 8 min	Heat bed B	3000	400	3000	400
8 to 16 min	Regenerate and Pulse	3012	166	4710	154
16 to 48 min	Cool bed B	28	13-1/2	28	13-1/2
48 to 53 min	Heat bed A	2000	400	3000	400
53 to 61 min	Regenerate and Pulse	3012	166	4710	166
61 to 90 min	Cool bed A	28	13-1/2	28	13-1/2
1 orbit	TOTAL	3012	1159	4710	1135
		Average Power = 772 watts		Average Power = 756 watts	

Although the average power requirement of the system is approximately 750 watts, higher peak power is required to heat the molecular sieve bed and pulse the Ohmjets. It should be noted, however, that all these peaks occur when the station is in the sun and therefore can come directly from the solar cells and not from the batteries. Since these peak loads do not exceed the normal excess power generated by the solar cells for charging the batteries, the maximum demands of the Ohmjet can be supplied simply by a temporary reduction of the charging rate of the batteries.

E. Weight Estimates -

The weight estimates for the components required for complete Ohmjet systems are given in Table III-2.

The total system weights include all components including additional electrical power system weight needed for the operation of one complete space station system, and does not include any extra components or subsystems which would be required for redundancy. Even if another complete system were added for 100 per cent redundancy, an Ohmjet system shows considerable weight savings compared to the 5840 lbs./year of bipropellant fuel ($I_{sp} = 300$ seconds) which would be required to do the same job.

Although Method II offers considerable weight savings as compared to Method I, for both Duty Cycles, the weight difference is not so decisive as to rule out Method I. However, factors such as reliability and simplicity make the use of Method II worthy of more detailed investigation.

F. Discussion -

Both methods of utilizing the waste CO_2 of the space station for attitude control investigated in this report are feasible and workable systems. Each method has certain advantages and disadvantages. These are listed below:

Method I - Compressing and storing CO_2 prior to use in the Ohmjet

Advantages

- (1) Smaller Ohmjet thrust unit required because of higher inlet pressure.
- (2) Smaller temperature rise required in the Ohmjet because of high compressor discharge temperature.
- (3) Storage tank acts as an accumulator to smooth over transient peaks and variations in CO_2 generation rate.

TABLE III-2, WEIGHT ESTIMATES FOR OHMJET SYSTEMS

ITEM	Weights in Pounds			
	METHOD I		METHOD II	
	Duty Cycle 1	Duty Cycle 2	Duty Cycle 1	Duty Cycle 2
Molecular Sieve Bed				
Bed Tank	N.C.*	N.C.	N.C.	N.C.
Bed Material (21.8# Linde Type 5A)	N.C.	N.C.	N.C.	N.C.
Heater	0.50#	0.40#	0.50#	0.40#
Insulation (1" of 3#/cu ft Foam)	2.56	2.56	2.56	2.56
Insulation cover (.010" Aluminum)	1.90	1.90	1.90	1.90
TOTAL Molecular Sieve Bed	4.96	4.86	4.96	4.86
Radiator				
Cooler Plate (0.080" Aluminum)	11.52	13.80	11.52	13.80
Tubes	1.44	1.73	1.44	1.73
Insulation (1" of 3#/cu ft Foam)	2.50	3.00	2.50	3.00
Insulation Cover (.010" Aluminum)	1.44	1.73	1.44	1.73
TOTAL Radiator	16.90	20.26	16.90	20.26
Circulating System				
Circulating Motor-Fan	0.41	0.50	0.41	0.50
V9 - 0.1" of H ₂ O check valve	0.20	0.25	0.20	0.25
Piping and Insulation	1.60	2.00	1.60	2.00
TOTAL Circulating System	2.21	2.75	2.21	2.75
Compressor System				
3 Stage 10:1 pressure ratio compressor	11.20	11.20		
Motor for compressor	2.20	1.40		
Insulation around compressor	0.60	0.60	--	--
Insulation cover (.01" Aluminum)	0.60	0.60	--	--
Piping and insulation (.15#/ft)	1.10	1.10	--	--
TOTAL Compressor System	14.70	13.90		
Storage Tank				
3 Ft ³ spherical tank	8.30	8.30	--	--
Insulation (2" of 3#/ft ³)	6.00	6.00		
Insulation cover (.010" Aluminum)	2.00	2.00		
TOTAL Storage Tank	16.30	16.30		
Valves and Remaining Piping and Insulation				
V ₁	N.C.*	N.C.	N.C.	N.C.
V ₂	N.C.	N.C.	N.C.	N.C.
V ₃ - 1/16" - 20 psia solenoid	0.40	0.40	0.40	0.40
V ₄ - 1/16" - 3 psi check relief	0.20	0.20	0.20	0.20
V ₆ - 1/4" - 20 psia - solenoid - 400°F	0.65	0.65	2.0	2.0
V ₇ - 1/8" - 150 psi - check, 1000°F	0.25	0.25	--	--
V ₈ - 1/16" - 150 psi solenoid, 1000°F	0.40	0.40	--	--
V ₉ - 100 psia pressure regulator, 1000°F	0.50	0.50	--	--
V ₁₀ - 1/8" - 150 psi - solenoid - 1000°F	1.00	1.00	--	--
Piping and Insulation (.15#/ft)	1.45	1.45	0.90	0.90
TOTAL, Valves and Remaining Piping	4.85	4.85	3.50	3.50

* N.C. - Denotes not chargeable to Ohmjet because item is required for life support.

TABLE III-2, WEIGHT ESTIMATES FOR OHMJET SYSTEMS (CONT'D)

ITEM	Weights in Pounds			
	METHOD I		METHOD II	
	Duty Cycle 1	Duty Cycle 2	Duty Cycle 1	Duty Cycle 2
Ohmjet				
Ohmjet Thrust Unit	2.0	2.0	4.0	4.0
Insulation	0.5	0.5	1.0	1.0
TOTAL OHMJET	2.5	2.5	5.0	5.0
Electrical Controls & Switchgear	15.0	15.0	10.0	10.0
TOTAL per Single System	77.4	80.4	42.6	46.4
TOTAL for the Two Systems Required (no redundancy)	155	161	85	93
Increase in Weight of Electrical Power System @ 350 #/kw	256	270	250	264
TOTAL Weight Attributable to Thrust System, lbs.	411	431	335	357

Disadvantages

- (1) Heavier.
- (2) Complex, requires more components such as compressor, storage tank, check valve and pressure regulator.
- (3) Ohmjet control valves must handle high pressure (150 psia) and high temperature (1000⁰ F.) gas.

Method II - Direct use of regenerated CO₂ from molecular sieve bed into the Ohmjet.

Advantages

- (1) Simple, requires only a few basic components.
- (2) Lighter weight.
- (3) Ohmjet valve must handle only low pressure (14.7 psia) and low temperature (392⁰ F.) gas.
- (4) The functional simplicity of Method II should lead to a higher reliability than that of Method I.

It is concluded that::

- (1) The Ohmjet thrust system is a simple, feasible and practical system for obtaining attitude control by the use of waste CO₂ from a manned space station.
- (2) Direct use of CO₂ during regeneration of a molecular sieve bed provides a simpler, lighter, and potentially more reliable system than one using a CO₂ compressor and storage tank.

IV DESIGN STUDIES OF A SOLAR-HEATED PULSE ROCKET (HELIOJET) THRUST SYSTEM

A. Design Requirements

The design concept of the Heliojet is to utilize a paraboloidal solar collector with a cavity receiver containing a heat exchanger, consisting of helical coils of metallic tubing. The unit is mounted on the sunward side of the space station so that the solar energy collected by the mirror is stored as thermal internal energy in the metallic heat exchanger tubes. Periodically, the propellant gas (in this case CO_2) is passed through the heat exchanger tubes where it is heated and then expanded through a nozzle to produce a thrust impulse.

A basic advantage of the Heliojet, as compared to the Ohmjet, stems from potentially higher efficiency due to the fact that solar energy is used to raise the propellant temperature directly, rather than through the intermediate process of converting solar energy to electrical energy. For the design study of the Heliojet, the same inlet conditions of the gas were assumed as for the Ohmjet and the objective has been to determine whether a realistic design configuration can be obtained with specific impulse comparable to that of the Ohmjet.

Based upon the studies in Section III, the following conditions were assumed for the CO_2 at the inlet to the Heliojet heat exchanger tubes:

Temperature----- 100°F

Pressure-----150 psia

Mach Number-----0.05

The above gives a gas velocity of 45 ft/sec and a density of 1.1 lbs/ft^3 . The corresponding mass velocity, G , is $49.5 \text{ lbs/ft}^2\text{-sec}$.

It was established that if the CO_2 production from 21 men were heated to 1600°F , the average rate at which impulse could be applied to the station would correspond to a continuous thrust of 0.0547 lbs. This produces two additional Heliojet design specifications: (1) The average gas temperature during the impulse must be about 1600°F . and (2) The average gas flow rate (lb/sec) must be such that an average thrust value of 0.0547 lbs is produced. It is to be noted that the latter specification is based upon the highest

rate of thrust application, i.e. when all of the available CO_2 is used for this purpose, which will occur during periods of maximum gravity gradient torque.

It is clear that the impulse duration is of primary importance in determining the average gas temperature attainable. Also, allowance must be made for the occurrence of eclipse during periods of maximum required thrust. Thus if we assume maximum eclipse time to be 35 minutes for an orbital period of 95 minutes, the thrust level must be increased by a factor of 1.585 so as to make up for the time in the dark when the Heliojet cannot operate.

Since the attitude control pulse must be applied at a predetermined angular orientation, the frequency of thrust application is related to the rate with which the station rotates about the sun-pointing axis. It will be assumed that this spin rate is 3 RPM. Hence, an impulse could be applied once every 20 seconds or at multiples of 20 second intervals, i.e., once every 40 sec., 60 sec., etc.

If thrust were to be applied once per rotation, the required impulse would

$$Ft = (0.0547) (20) (1.585) = 1.735 \text{ lb-sec per rotation} \quad (1)$$

It will be assumed that the design thrust level is 1.735 lbs. This permits a choice of t , the thrust duration, depending upon the frequency of thrust application. Thus, if the impulse is applied once every rotation, $t=1$ sec., if applied every 40 seconds, $t = 2$ sec. A thrust duration much longer than 2 seconds is not as efficient in that the average moment arm of the thrust is reduced as the angular firing angle exceeds 36° .

The various requirements which the Heliojet design must meet can be further defined as follows:

(a) Since allowance should be made for prolonged periods of time in sunlight without thrust application, the maximum heat exchanger temperature must be kept to a reasonable value so as not to damage the unit. If we assume the tubes and cavity liner to be made of Niobium, thus temperature should not exceed 2500°F . This requirement is used to limit the concentration ratio of the solar collector.

(b) During CO_2 flow, the gas temperature at the exit of the heat exchanger tubes must average 1600°F . in order to produce the desired specific impulse of 120 sec. This requirement is the principal consideration in the analysis of transient heat-transfer from the tube walls to the gas.

- (c) In the time available between thrust application the tube wall temperature must rise to an initial temperature high enough to be consistent with (b) above.
- (d) Collector and cavity geometry must permit angular misalignments with respect to the sun of one degree or more without affecting operation of the system.

In order to define the design of a Heliojet thrust system, analyses were performed in three separate areas: optical design, receiver heat-up rates, and transient heat-transfer to the gas. These are described below, followed by a description of a configuration meeting the various requirements defined.

B. Optical Design Considerations

(1) Concentration Ratio

Since the exterior of the cavity will be insulated to minimize heat loss from the walls, and since precautions will be taken in the design to limit losses due to direct reflection from the cavity opening to less than 2 per cent, the heat balance equation can be written as:

$$Q_s A_p - A_c \sigma T^4 = W C_p \frac{dT}{dt} \quad (2)$$

where

Q_s - Solar heat flux = 442 BTU/hr-ft²

A_p - Area of paraboloid

A_c - Area of cavity opening

T - Heat-exchanger tube wall temperature, °R

σ - Stefan Boltzman constant = $0.174 \times 10^{-8} \frac{\text{BTU}}{\text{hr-ft}^2 (\text{°R})^4}$

W - weight of receiver tube walls, lbs.

C_p - specific heat of tube material, BTU/lb. -°F.

The maximum receiver temperature will be reached in the steady-state, i.e. when $dT/dt = 0$. Hence

$$T_{\max} = \left[\frac{(Q_s)(A_p)}{(\sigma)(A_c)} \right]^{1/4} \quad (3)$$

Since A_p/A_c defines the concentration ratio, C , its value can be determined for a given value of T_{\max} .

For $T_{\max} = 2,500^\circ\text{F.} (2,960^\circ\text{R})$, the maximum allowable concentration ratio is:

$$\frac{A_p}{A_c} = C = 300 \quad (4)$$

(2) Losses due to reflection -

In order to approximate a black-body cavity absorber, the amount of radiation passing directly out of the cavity opening after reflection from interior surfaces must be minimized. This is accomplished by making the ratio of cavity aperture area A_c to cavity internal surface area A_i as small as possible. As shown in Reference IV-1, when this ratio is of the order of 0.02, the fraction of light passing directly out of the opening would be about 2 percent. This fraction is, for all practical purposes, independent of cavity geometry, i.e. whether conical, spherical or cylindrical in shape. It is also not appreciably affected by the value of interior surface emittance if the latter is in the range of 0.3 to 1.0 over all wave lengths.

In the Heliojet design, the total internal area of the cavity is made up of the cavity wall and the exterior of the heat exchanger tubes. It is assumed that these tubes will be spaced apart by one tube diameter in order to permit reflected radiation within the cavity to heat the tube wall uniformly on all sides.

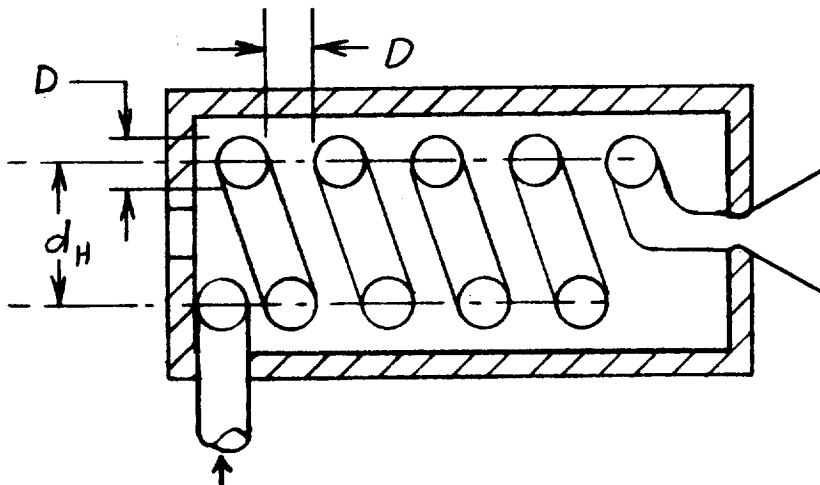


Figure IV-1 Geometry of Heat Exchanger Tube

Since the cavity diameter is approximately equal to the coil diameter d_h ,

$$A_i = \pi^2 D d_h N + 2\pi D d_h N \quad (5)$$

where N = number of helical turns

The first term above represents the tube heat transfer area A_{HT}

Hence

$$A_i = A_{HT} + \frac{2}{\pi} A_{HT} = 1.64 A_{HT} \quad (6)$$

In order that

$$\frac{A_c}{A_i} \leq 0.02$$

It is necessary that

$$\frac{A_c}{A_{HT}} \leq (1.64)(0.02) = 0.033$$

For design purposes a value of $A_c/A_{HT} = 0.03$ will be used. This will maintain losses due to direct reflection to less than 2 percent (Ref. IV-1).

(3) Angular misalignments -

Reference IV-2 provides the basic relationships and criteria for estimating the amount of angular misalignment which can be tolerated for a given size cavity. For nomenclature as shown in Figure 2, pertinent relationships are summarized in Fig. IV-2.

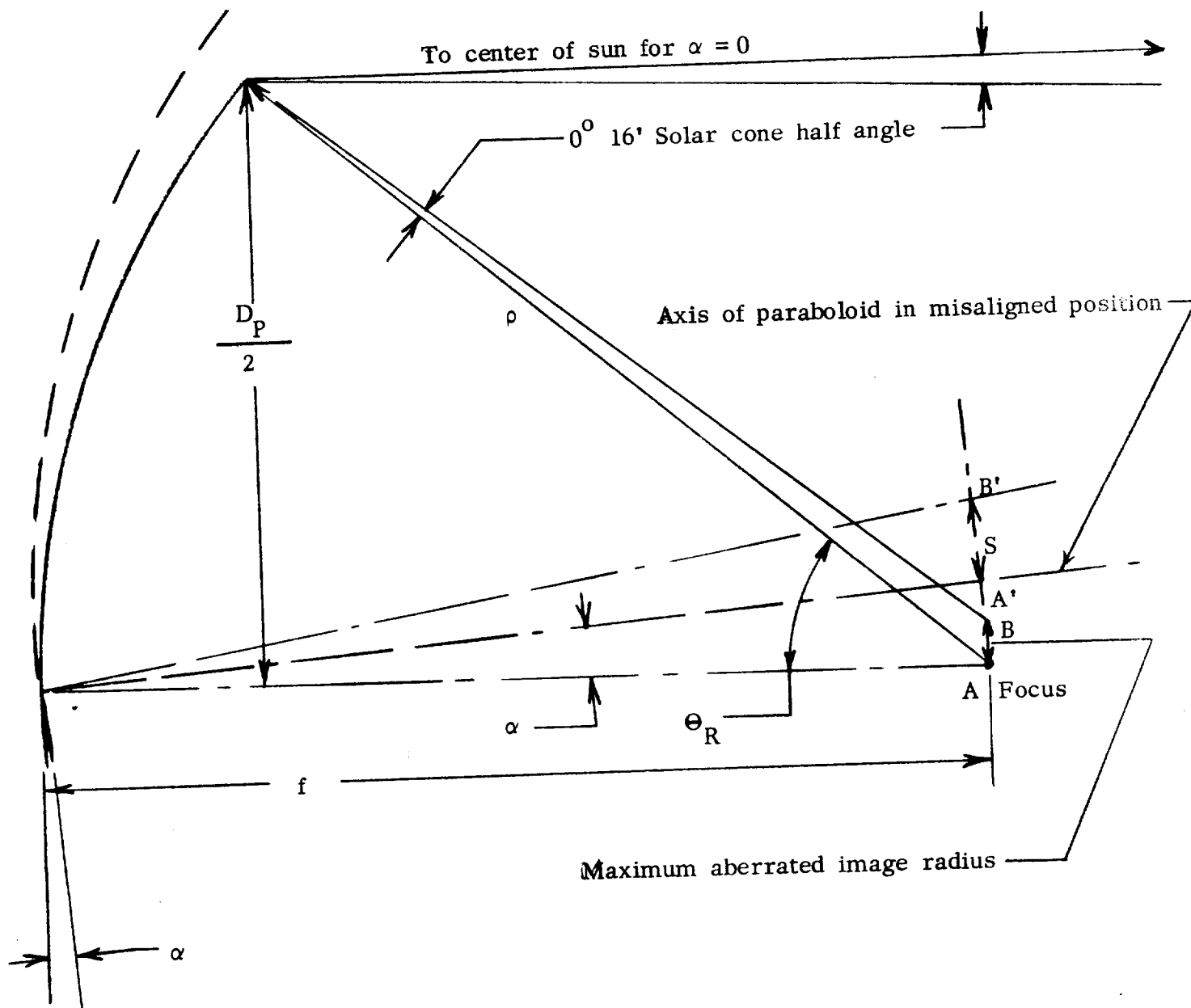
$$\rho = \frac{2f}{1 + \cos \Theta_R} \quad (8)$$

$$f = \frac{D_p (1 + \cos \Theta_R)}{4 \sin \Theta_R} \quad (9)$$

$$\rho = \frac{D_p}{2 \sin \Theta_R} \quad (10)$$

$$r_a = \frac{0.00931 f}{(1 + \cos \Theta_R) \cos \Theta_R} \quad (11)$$

$$\frac{S}{\alpha} = \frac{2\rho - f}{\cos \Theta_R} = \frac{D_p (3 - \cos \Theta_R)}{2 \sin 2\Theta_R} \quad (12)$$



SOLAR COLLECTOR GEOMETRY

FIGURE IV - 2

The distance S in equation (12) is the maximum motion, relative to the center of the circular solar image, of a point in the focal plane reflecting from the rim of the mirror due to a misalignment angle α with respect to the sun. To minimize motion of the image it is desirable to choose a value for the rim angle, Θ_r , at which

$$\frac{d(S/\alpha)}{d\Theta_r} = 0$$

The corresponding value of the rim angle is $\Theta_r = 42^\circ$. This value is therefore used to define the geometry of the paraboloid.

According to Reference IV-2, the energy distribution within the aberrated solar image can be approximated by assuming it to be of constant intensity within the circular solar image and then falling off linearly until it reaches zero intensity at $r = r_a$. On this basis, the image which is to be confined within the cavity aperture has a radius r_a given by equation (11). In terms of the diameter D_p and for $\Theta_r = 42^\circ$, this becomes -

$$r_a = 0.00467 D_p \quad (13)$$

The angle α at which r_a will reach the edge of the cavity aperture and still be confined within it is found from

$$r_c = S + r_a \quad (14)$$

which for $\Theta_r = 42^\circ$ yields

$$\alpha = 50.6 \left(\frac{r_c}{D_p} \right) - 0.236 \text{ (degrees)} \quad (15)$$

Having fixed the concentration ratio at 300, the ratio $\frac{r_c}{D_p}$ in equation (15) also becomes fixed. Thus

$$\frac{r_c}{D_p} = \frac{1}{34.7}$$

and the misalignment angle which can be accepted without affecting operation of the solar heating system is

$$\alpha_{\max} = 1.22 \text{ degrees}$$

C. Receiver Heat-Up Rates -

The rate at which the heat-exchanger wall temperature will rise during the time when there is no propellant flow can be calculated from equation (2):

$$\frac{dT}{dt} = \frac{Q_s A_p}{\rho \delta C_p A_{HT}} \left[1 - \frac{(\sigma / Q_s) T^4}{(A_p / A_C)} \right] \quad (18)$$

The concentration ratio A_p / A_C has been previously selected to be 300. The ratio A_C / A_{HT} has been selected to be 0.03. Hence

$$\frac{A_p}{A_{HT}} = \frac{300 A_C}{A_{HT}} = (0.03) (300) = 9 \quad (19)$$

For tubes made out of Niobium to withstand the maximum temperature of $2,500^\circ \text{F}$,

$$C_p = 0.1 \text{ BTU/lb} - ^\circ \text{F}$$

$$\rho = 524 \text{ lbs/ft}^3$$

Equation (18) becomes

$$\frac{dT}{dt} = \frac{253}{\delta_m} \left[1 - 0.0131 \left(\frac{T}{1000} \right)^4 \right] \quad (20)$$

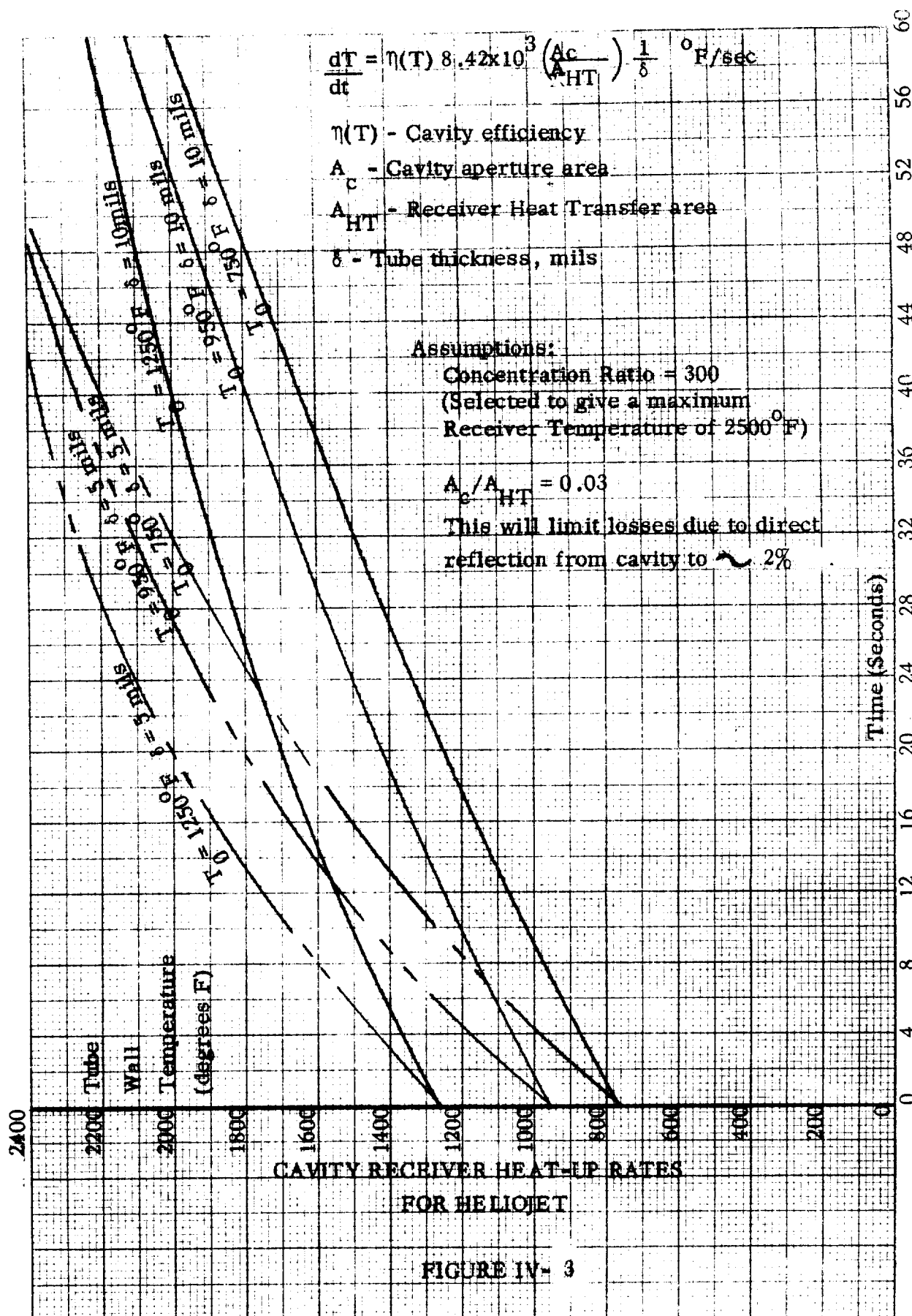
where δ_m = wall thickness in thousands of an inch (mils)

For the present purpose, an explicit integration of equation (20) is not warranted.

To obtain the variation of wall temperature with time for assumed initial temperatures T_0 and wall thickness δ_m , a step-wise numerical process was used. It was assumed $\frac{dT}{dt}$ is constant over temperature intervals of $\pm 50^\circ \text{F}$. around the value of T for which $\frac{dT}{dt}$ is computed. Results are plotted in Figure IV-3 for assumed initial temperatures of 750°F ., 950°F . and $1,250^\circ \text{F}$. For each of these values, the temperature rise is shown for wall thickness of 5 and 10 mils.

It is evident from Figure IV-3 that if the wall temperature is to rise to a value substantially above $1,600^\circ \text{F}$. in one or two revolutions of the station, the initial temperature (at the end of a gas flow pulse) must be in the order of $1,250^\circ \text{F}$. If operation of the Heliojet is to occur once every rotation of the station, i.e. every 20 seconds, a wall thickness of 5 mils will be required to reach a temperature of about $1,950^\circ \text{F}$. Similarly, if thrust is to be applied every two rotations, the same temperature could be reached with a wall thickness of 10 mils.

Without increasing the thrust level beyond the assumed value of 1.735 lbs., the greatest flexibility in programming the frequency of applied impulses will be obtained if it is possible to actuate the Heliojet every rotation of the station. For this reason a wall thickness of 5 mils is chosen.



D. Transient Heat-Transfer Analysis

Appendix A contains a detailed description of the transient heat-transfer analysis and provides relationships for the variation of gas and wall temperature with time and as a function of the various design parameters. Figures A-2 and A-3 of the above appendix give dimensionless design curves for the gas and wall temperatures, respectively. These curves provide a means for selecting the diameter and length of the heat exchanger tubing and the thrust duration. The procedure is essentially one of trial and error, for the values ultimately chosen must meet the requirements for wall temperature described in the preceding section and must also match the design curves for both wall and gas temperature during transient heat-transfer. One set of values which meets these conditions has been found to be:

Tube inside diameter - $D = 0.10$ inches

Length of one tube - $L = 30$ inches

Pulse duration - $t =$ one second

Referring to Figures A-2 and A-3 of Appendix A, the above design assumptions yield the following values for the coefficients K_2 & K_3 :

$$K_2 = 4 \text{ St} \left(\frac{L}{D} \right) = 4.42 \quad (21)$$

$$K_3 = \text{St} \left(\frac{C_{ps}}{C_{pw}} \right) \left(\frac{G}{\rho \delta} \right) = 2.06 \quad (22)$$

The Stanton Number (St) has been evaluated in accordance with the relationships defined in Appendix A; all other parameters have been selected in the preceding sections. Using the above:

$$\frac{\Delta T_{wa}}{T_{wa}(t) - 100} = \frac{1970 - 100}{1970 - 100} = 0.63 \quad (23)$$

This yields an average wall temperature at the end of the one second impulse of

$$T_{wa}(1) = 1,275^\circ\text{F}.$$

This value, and the initial value of $T_{wo} = 1970^\circ\text{F}$. used in equation (23), match the initial and final conditions of temperature rise during the tube-wall cycle (See Figure IV-3 for $\delta = 5$ mils).

The highest gas exit temperature, reached at the start of the impulse, is found from the value of $\overline{\Delta T}_{ge}$ at $t = 0$. This yields

$$\frac{\overline{\Delta T}_{ge}}{1970 - 100} = \frac{T_{ge}(0) - 100}{1970 - 100} = 1 - e^{-4.42} = 0.988 \quad (24)$$

Hence,

$$T_{ge}(0) = 1945^{\circ}\text{F}.$$

Exit gas temperature at the end of the one second impulse is found from

$$\Delta T_{ge}(1) = \frac{T_{ge}(1) - 100}{1970 - 100} = 0.625 \quad (25)$$

$$T_{ge}(1) = 1270^{\circ}\text{F}$$

(It is to be noted that this value of gas temperature cannot be compared directly with the average wall temperature of $1,275^{\circ}\text{F}$. since the latter represents an average over the tube length. See Appendix A for further discussion.)

The average value of gas exit temperature during the impulse is therefore

$$\frac{1945 + 1270}{2} = 1607^{\circ}\text{F}$$

The average value of gas exit temperature needed to produce the assumed specific impulse of 120 seconds is $1,600^{\circ}\text{F}$.

E. Heliojet Configuration

The preceding analysis establishes the length and diameter of the tubing in the Heliojet heat exchanger: $L/D = 300$, $D = 0.1"$, $L = 30"$. However, the diameter thus chosen will not accomodate the required mass flow in one tube. The number of parallel tubes needed is found from

$$A_F = N \frac{\pi}{4} D^2 = \frac{w_a}{G} \quad (26)$$

where N = number of tubes

$$\text{since } w_a = \frac{F}{I_{sp}} = \frac{1.735}{120} = 0.01448 \text{ lb/sec} \quad (27)$$

and $G = 49.5 \text{ lb/ft}^2 - \text{sec}$

The above yields

$$N = 5.36$$

To produce a round number of tubes, say $N = 5$, the diameter should be 0.1035" rather than the value of 0.100" previously used. This small change does not appreciably affect the preceding calculations because D enters through the Stanton number both into the calculations of K_2 as well as K_3 . However, L/D must be maintained at 300 since it enters only into K_2 . To do this the length of each tube is increased to

$$L = (300)(0.1035) = 31.1 \text{ inches}$$

Using five tubes in parallel wound on a 3" diameter helix results in a heat exchanger as shown in Figure IV-4. Also shown are related sizes of the concentrator and cavity based upon the design criteria described in preceding sections.

F. Weight Estimates

The estimated weight breakdown of the Heliojet thrust unit shown in Figure IV-3 is shown in Table I.

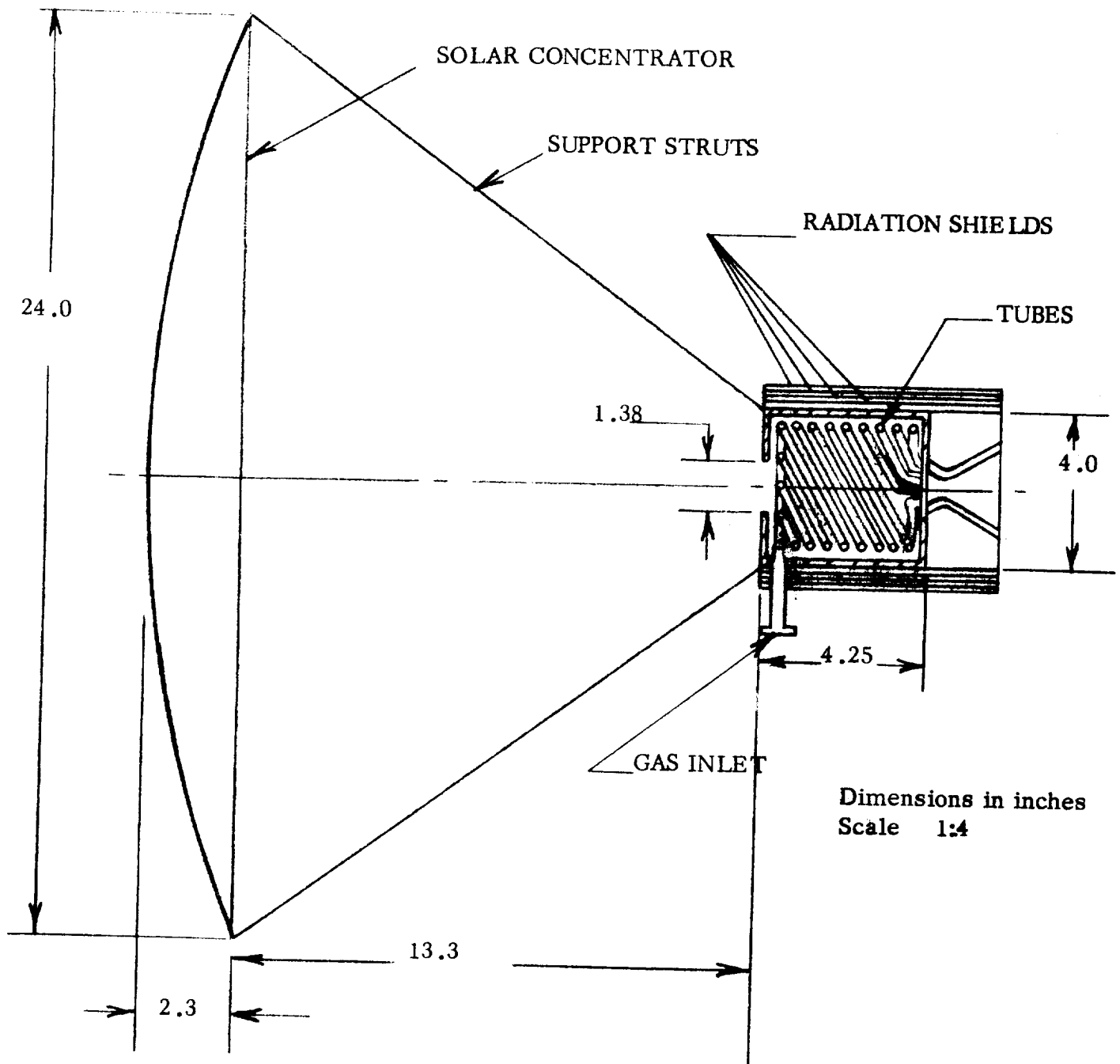
Table I - Estimated Weight Breakdown of Heliojet Thrust Unit

Concentrator mirror (2 ft. diam.)	1.5 lbs.
Cavity Structure - 0.020" Niobium walls and radiation shielding	0.5 lbs.
Heat exchanger tubing	0.1 lbs.
Nozzle	0.2 lbs.
Concentrator support structure	<u>0.7 lbs.</u>
Total Thrust Unit Weight	3.0 lbs.

The weight of the CO_2 recovery and storage equipment for a Heliojet thrust system is estimated on the basis of calculations made (see Section III) for an Ohmjet system, using Method I, i.e. using a compressor and storage tank to recover CO_2 at a pressure of 10 atmospheres. Since the Heliojet uses CO_2 every 20 or 40 seconds

as the space station is in sunlight, it is necessary to store CO_2 during periods between regeneration of the molecular sieve beds. It is assumed that two sieve beds are used and each is regenerated once per orbit. It is conservatively assumed that heat losses will occur from the storage tanks so that the Heliojet inlet temperature is only 100°F . even though the compressor discharges CO_2 into the storage tank at 1000°F .

The estimated weight of components for a complete Heliojet system is shown in Table IV-2.



Concentration Ratio : 300

Internal Cavity Design:

5 Tubes in parallel. Tube Material: Niobium.

Tube ID: 0.104 inch. Wall Thickness: 0.005 inch.

Tubes are wound on a 3.0 inch diameter helix with 0.114 inch spacing between adjacent tubes. Developed

length of each tube is 31 inches. Number of turns: 3.4 per tube. Total no. of turns: 17.

CONFIGURATION OF HELIOJET THRUST UNIT

FIGURE IV- 4

Table IV-2

Estimated Weight Breakdown of Heliojet Thrust System

	Weight (lbs)
Two Solar-heated thrust units	6.0
Two Heaters and Insulation for molecular sieve beds	10.0
Two Radiators to cool sieve beds	40.0
Two circulating systems to cool sieve beds	5.5
Two compressor systems	28.0
Two CO ₂ storage tanks	32.6
Valves and piping	9.7
Electrical controls for valves	<u>6.0</u>
Total Heliojet System (no redundancy)	137.8 lbs

G. Conclusions

1. In order to compensate for the maximum anticipated gravity gradient torque by the use of a solar heated pulse rocket (Heliojet), it is desirable to design for a single thrust impulse to be delivered every one or two rotations of a space station while it is in sunlight. If corrections are made less frequently, the size of the solar collector would become excessive. The Heliojet system requires that carbon dioxide be recovered, compressed and stored so that it may be used every 20 or 40 seconds during periods of maximum torque requirement.

2. The Heliojet system analyzed above when operated on every rotation of the station produces the same performance as an Ohmjet system which is electrically heated to 1600°F. During periods of less than maximum torque requirement, the same Heliojet design may have a longer heat up time and would achieve higher average nozzle inlet temperatures. It has been estimated that if thrust is applied every two rotations, the average nozzle inlet temperature would be 1900°F., leading to a 10 percent increase in specific impulse to 130 seconds, as compared to 120 seconds for the reference design.

3. Operation of a Heliojet system requires that the space station spin vector be oriented to the sun with an accuracy of $\pm 1.25^\circ$.

4. The estimated Heliojet unit weight of three pounds is low enough that two or more units could be used for redundancy.

5. The estimated concentrator diameter of two feet is small enough to permit a simple one-piece mirror construction and the required concentration ratio of 300 will be easily achievable. (Concentration ratios of 1000 or more are required for solar-thermionic power systems).

V EXPERIMENTAL TESTING OF OHMJET THRUST UNIT

A. Test Objectives -

The objectives of the experimental test program were to determine the thrust, specific impulse, and total impulse per pulse for an Ohmjet thrust unit operating with carbon dioxide as the propellant. During the test program, it became apparent that the nozzle inlet temperature was a sensitive function of the heat transfer coefficient from the helical heater wire to the gas, for which no prior empirical data were available. Therefore, preliminary measurements were made to determine the heat transfer coefficients, as well as the electrical efficiency for steady state operating conditions.

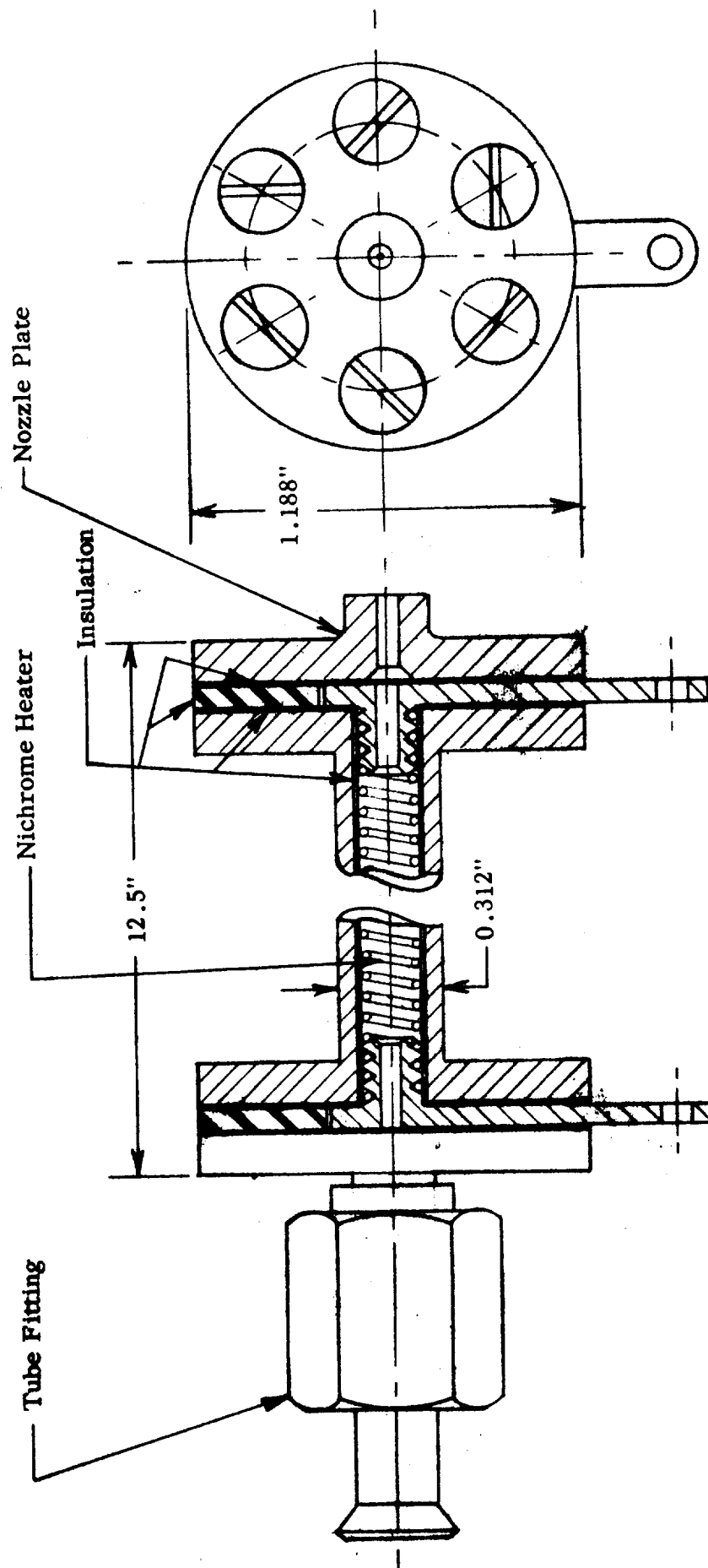
B. Description of Ohmjet Unit -

Figure V - 1 shows a drawing of the Ohmjet unit used in the test program. It consists of a tubular stainless steel chamber with a replaceable converging orifice as the nozzle, an internal helix of Nichrome wire as the heater element which is electrically and thermally insulated from the tube wall by a sheet of flexible asbestos paper, and electrical bus-bar connections to permit application of up to 220 volt, 60 cycle power to the heater element.

The unit was designed for a CO_2 inlet pressure of 150 to 200 psia and to operate with heater element temperatures up to 1850°F . and nozzle inlet temperatures up to 1600°F . The nozzle plate used in the experiments had a converging orifice with a throat diameter of 0.0625 inch which exhausted to the atmosphere.

Carbon dioxide was supplied to the Ohmjet from a pressure tank by a pressure regulator and the flow was controlled at the inlet to the Ohmjet by a fast-acting solenoid valve (Marotta Valve Company Number MV-100) which had been modified to attain an opening time and closing time of approximately 10 milliseconds.

The heater coil consisted of a helix of 20 mil diameter Nichrome V wire with an outside coil diameter of 0.180 inch and approximately 300 turns between the electrical contacts. The resistance of the heater at 70°F . was measured to be 22.55 ohms. Therefore, upon rapid application of 220 volts, the initial current was 9.75 amperes and the initial power, 2150 watts. The mass of the heater coil between contacts was calculated to be approximately 6.6 grams. Assuming a specific heat for Nichrome of $0.11 \text{ cal/gm}^\circ \text{C}$, the initial heating rate with 220 volts would be:



OHMJET THRUST UNIT

Figure V - 1

$$\frac{dT}{dt} = \frac{P}{WC_p} = \frac{2150(0.2388)}{(6.6)(0.11)} = 780^{\circ} \text{ C/sec} = 1400^{\circ} \text{ F/sec.}$$

C. Discussion of Ohmjet Testing under Pulsed Operating Conditions -

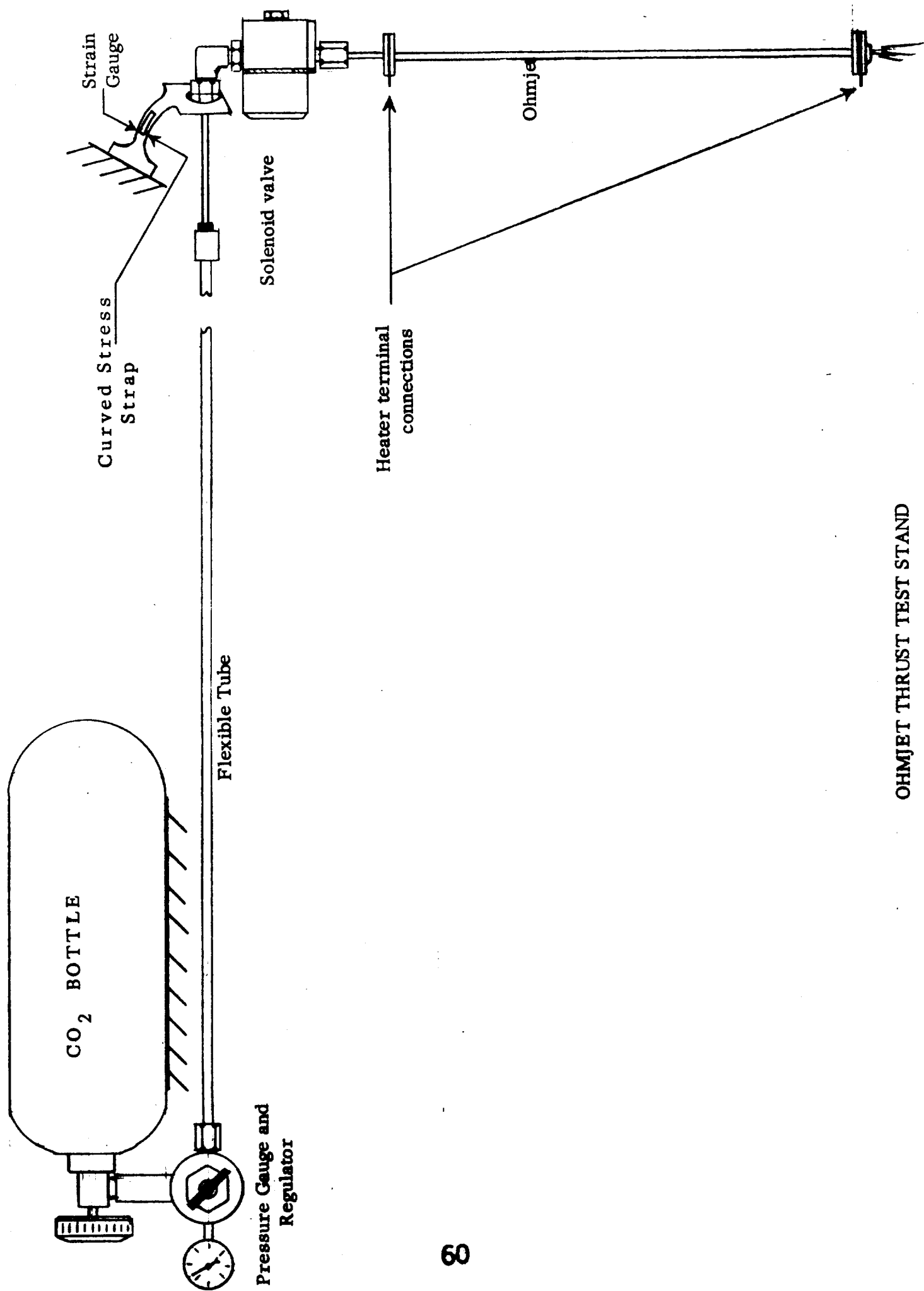
The measurement of transient thrust levels below one pound with rise times of the order of 10 milliseconds poses severe problems in achieving adequate sensitivity and avoiding ringing and overshoot in recording the thrust vs time curves. A reasonably satisfactory method was achieved in the following manner.

As shown in Figure V - 2 and V - 3, the Ohmjet thrust unit with its control valve attached was suspended on a thin elastically bent strip of stainless steel, 0.010" thick by 0.500" wide by 2.0" long which had strain gages (Baldwin Lima Hamilton Number C-14) mounted on each side. One strain gage was connected in a bridge circuit having a DC applied voltage of 90 volts. The output of the bridge was amplified in a high gain DC amplifier (Tektronix Model D) and applied to the vertical deflection plates of a Tektronix Model 531A oscilloscope.

Carbon dioxide was supplied at a regulated pressure up to 150 psig through a long flexible tube to the inlet port of the control valve. The control valve was actuated by a 24 volt DC power supply with opening and closing times programmed by a mechanical switch programmer (Eagle Model A6). When the control valve was opened, the thrust developed by the Ohmjet reduced the weight of the Ohmjet unit applied to the strain gage element and the thrust time curve was recorded on the oscilloscope as shown in Figures V - 4 and V - 5.

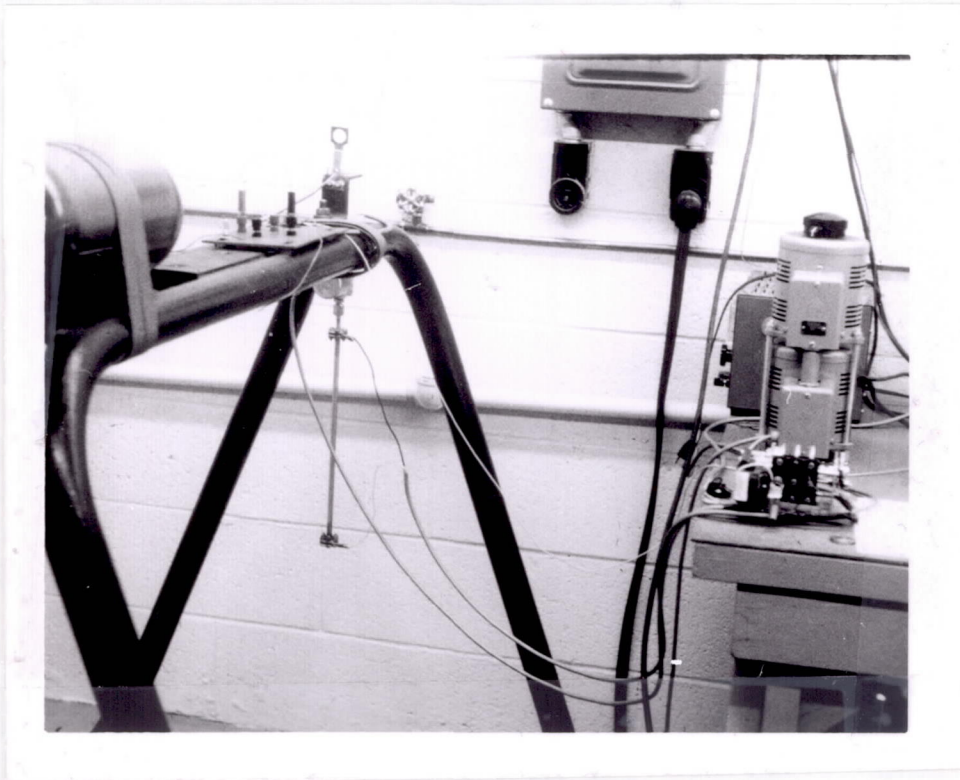
The strain gage system was calibrated statically by applying a vertical upward force on the Ohmjet with a spring balance and observing the resultant oscilloscope deflection. The calibration curve is shown in Figure V - 6.

With the stainless steel suspension strip initially bent to the degree necessary to obtain adequate bending stress in the strain gage to measure thrust levels of less than one pound, it was found that the natural frequency of the suspension system for vertical vibrations was approximately 10 cps. The 10 cps ringing oscillations shown in Figure V - 4 were induced by the rapid application of thrust with insufficient system damping. In these tests a small piston and cylinder dashpot filled with air was connected to the Ohmjet to introduce damping by viscous and sliding friction. However, with this design it was not possible to achieve a large fraction of critical damping, even with water in the dashpot.



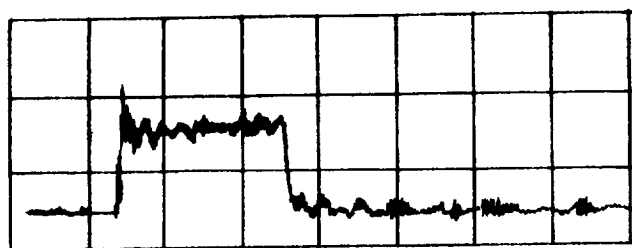
OHMJET THRUST TEST STAND

Figure V - 2



PHOTOGRAPH OF OHMJET THRUST TEST STAND

FIGURE V - 3



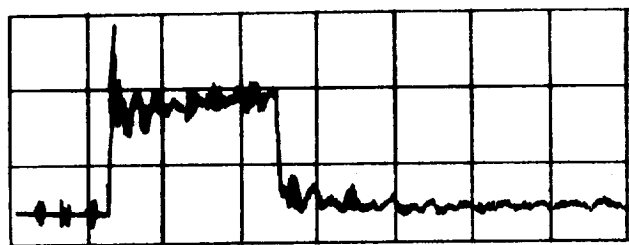
Nozzle Throat Diameter = 1/16 in.

Average Thrust = 0.31 pound

Duration = 1.2 seconds

THRUST - TIME RECORD AT 125 psig REGULATED PRESSURE

FIGURE V - 4



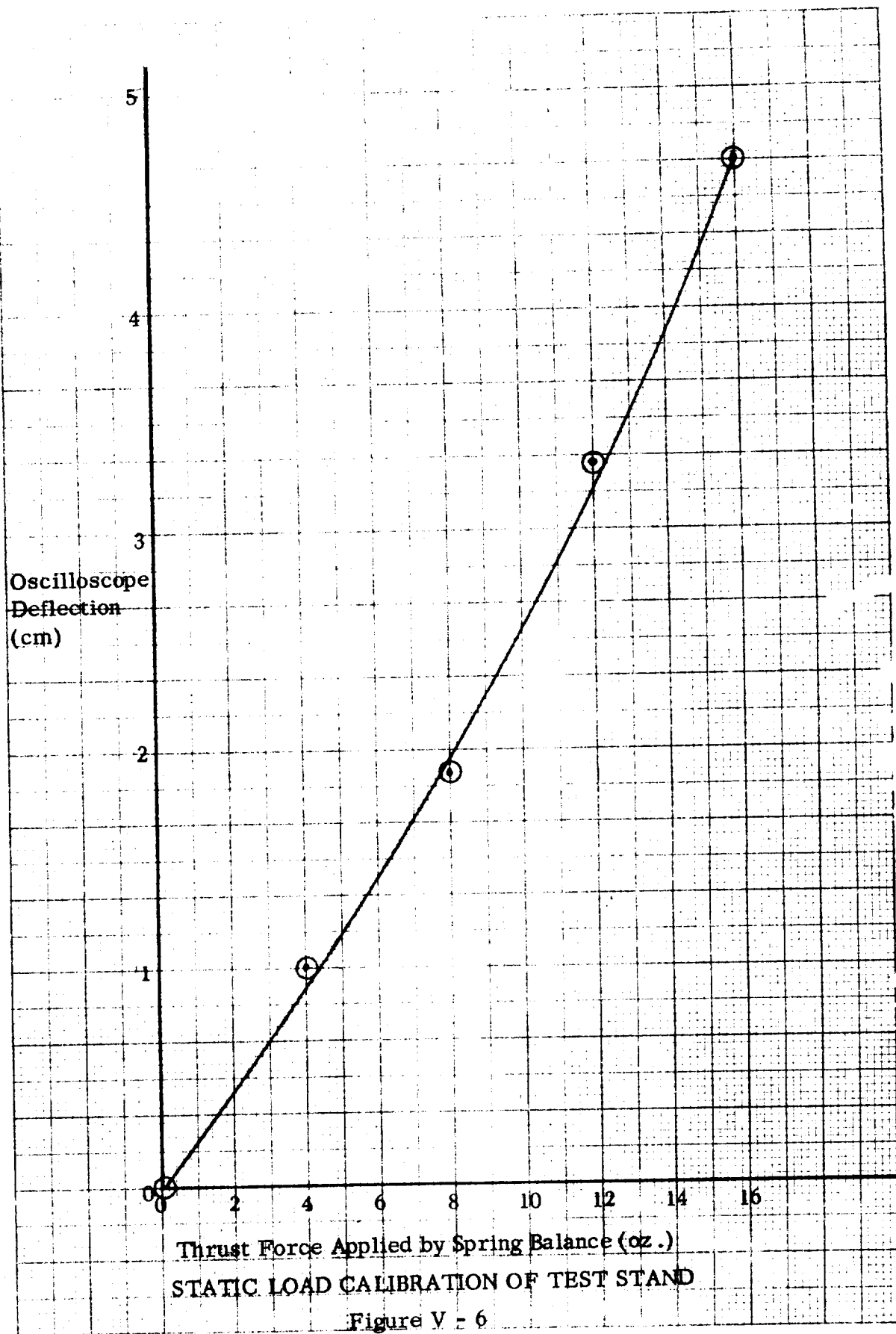
Nozzle Throat Diameter = 1/16 in.

Average Thrust = 0.375 pound

Duration = 1.2 seconds

THRUST - TIME RECORD AT 150 psig REGULATED PRESSURE

FIGURE V - 5



Therefore, all oscillograms obtained exhibited some degree of initial overshoot and ringing. However, the average amplitude of the thrust and the total pulse duration were quite accurately repeatable from one pulse to the next.

By comparing measured thrust levels with the thrust calculated on the basis of throat area, nozzle inlet pressure, and orifice thrust coefficient, it was estimated that the pressure drop from the regulator through the control valve and the Ohmjet heat exchanger section was approximately 28 per cent of the upstream regulated pressure for the test conditions of Figures V-4 and V-5.

Transient tests were made with electrical power up to 200 volts applied to the Ohmjet for one to 2 seconds prior to opening of the gas valve, followed by continued power and flow for pulse durations of 1.2 seconds. Because of the low gas discharge temperatures attained and the limitations on accuracy of thrust measurement, the thrust-time records were essentially the same for hot flow as for cold flow tests.

D. Discussion of Ohmjet Testing Under Steady State Operating Conditions -

In order to obtain data on electrical efficiency and heat transfer coefficients, a series of tests were made with the Ohmjet operating at steady state flow conditions. Measurements were made of the inlet pressure, P_{01} , the jet discharge total temperature, T_{02} , and the maximum wall temperature, T_{WM} , of the Nichrome heater element.

The inlet pressure was measured with a Bourdon pressure gage (0 to 100 psig). The exit total temperature was measured by impinging the jet into a stagnation cup which was 2 inches in diameter by 3 inches deep in which a radiation-shielded Chromel-Alumel thermocouple was located. The maximum Nichrome heater temperature for each run was estimated in the following way. By visual sighting at a slight angle up through the Ohmjet nozzle, the heater could be seen and compared in color temperature to that of a 150 watt tungsten bulb. The applied voltage to the bulb filament was adjusted to achieve color match and the temperature of the filament was determined from a calibration of voltage against filament temperature as read by a Pyro-Micro Optical Pyrometer (Model 95).

The experimental data obtained are shown in Table V-1. Measurements were made at applied voltages up to 235 volts with exit CO_2 temperatures up to $555^{\circ}F$. and inlet pressures up to 91 psig. The electrical power input for each point was calculated from the measured voltage by using the measured room temperature resistance of 22.55 ohms. and assuming a temperature coefficient of resistivity for Nichrome of 0.0004 per $^{\circ}C$.

TABLE V-1

EXPERIMENTAL DATA ON OHMJET WITH CO₂ AT STEADY STATE FLOW CONDITIONS

Applied Voltage (volts)	Inlet Pressure (psig)	Inlet Temp °F	Exit Total Temp °F	Max. Nichrome Temp °F	Calculated Power Input (watts)	Mass Flow Rate lb/sec x 10 ⁻³	Electrical Efficiency %	Heat Transfer Coefficient Btu/ft ² -sec °F x 10 ⁻³
0	20	60	60	60	0	2.97	-	-
140	20	60	320	2000	608	2.41	25	2.6
140	40	40	290	1350	675	3.88	32	5.9
140	51	40	280	1000	718	4.63	34	9.9
165	62	40	330	1250	955	5.27	39	11.7
182	62	40	370	1800	1060	5.13	39	8.3
193	62	40	400	2100	1134	7.07	54.5	10.5
193	90	30	355	1450	1260	6.89	43	14.3
214	91	30	420	1900	1440	6.40	42	11.8
235	91	30	555	2600	1565	6.30	55	11.3
0	76	30	30	30	0	-	-	-
170	21	30	440	2500	632	2.31	28	3.2
180	21	30	Burn Out	Burn Out	828	-	-	-

Figure V-7 shows the experimental data on CO₂ discharge total temperature vs. electrical power input for a range of inlet pressures from 35 to 105 psia.

For many of the test conditions, about half the length of the Ohmjet was observed to glow cherry red. No thermal insulation was used to reduce radiative or convective heat losses. After 13 successful test runs, the Nichrome heater was inadvertently burned out at an applied voltage of 180 volts and an inlet pressure of 21 psig. The Nichrome failed at a point about 1.2 inches upstream from the nozzle. Inspection showed some damage to the rear bus-bar and nozzle inlet, probably initiated by fragments or droplets of Nichrome which produced an electrical short.

Since the mass flow rate was not measured directly, the data were reduced using the assumptions: (1) that the drop in total pressure through the Ohmjet heat exchanger section is negligible and (2) that the mass flow rate corresponds to choked flow (Mach 1) through a 1/16 inch diameter orifice at a total pressure equal to the measured inlet pressure and a total temperature equal to the measured exit total temperature. With these assumptions, the mass flow rate (w) for each test point was calculated from the equations:

$$\frac{w \sqrt{T_{02}}}{A_{TH} P_{02}} = 0.63 \text{ } ^\circ R^{1/2} / \text{sec. for CO}_2 \text{ (K=1.25)}$$

with $P_{02} = P_{01}$ and $A_{TH} = \text{throat area} = 2.13 \times 10^{-5} \text{ ft.}^2$

The power input to the gas was calculated from

$$q_G = w \bar{C}_p (T_{02} - T_{01})$$

where $\bar{C}_p = \text{average specific heat of CO}_2 = 0.23 \text{ Btu/lb. } ^\circ F.$

The electrical efficiency was calculated from

$$\eta_E = \frac{q_G}{q_E} = \frac{w \bar{C}_p (T_{02} - T_{01})}{q_E}$$

where $q_E = \text{electrical power input, Btu/sec.}$

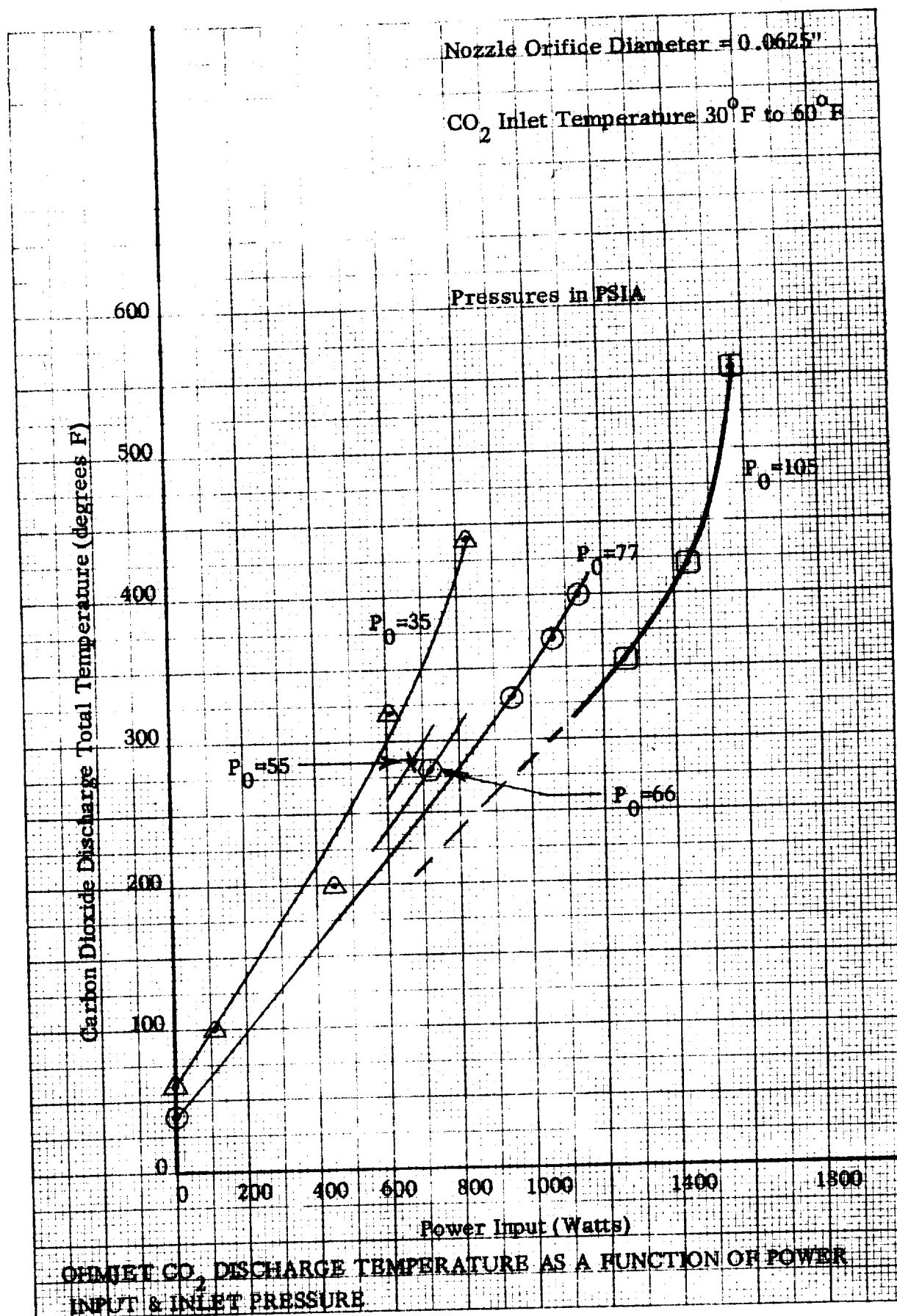


FIGURE V-7

The heat transfer coefficient was defined and calculated from

$$h = \frac{q_G}{A_{HT} \Delta T_F}$$

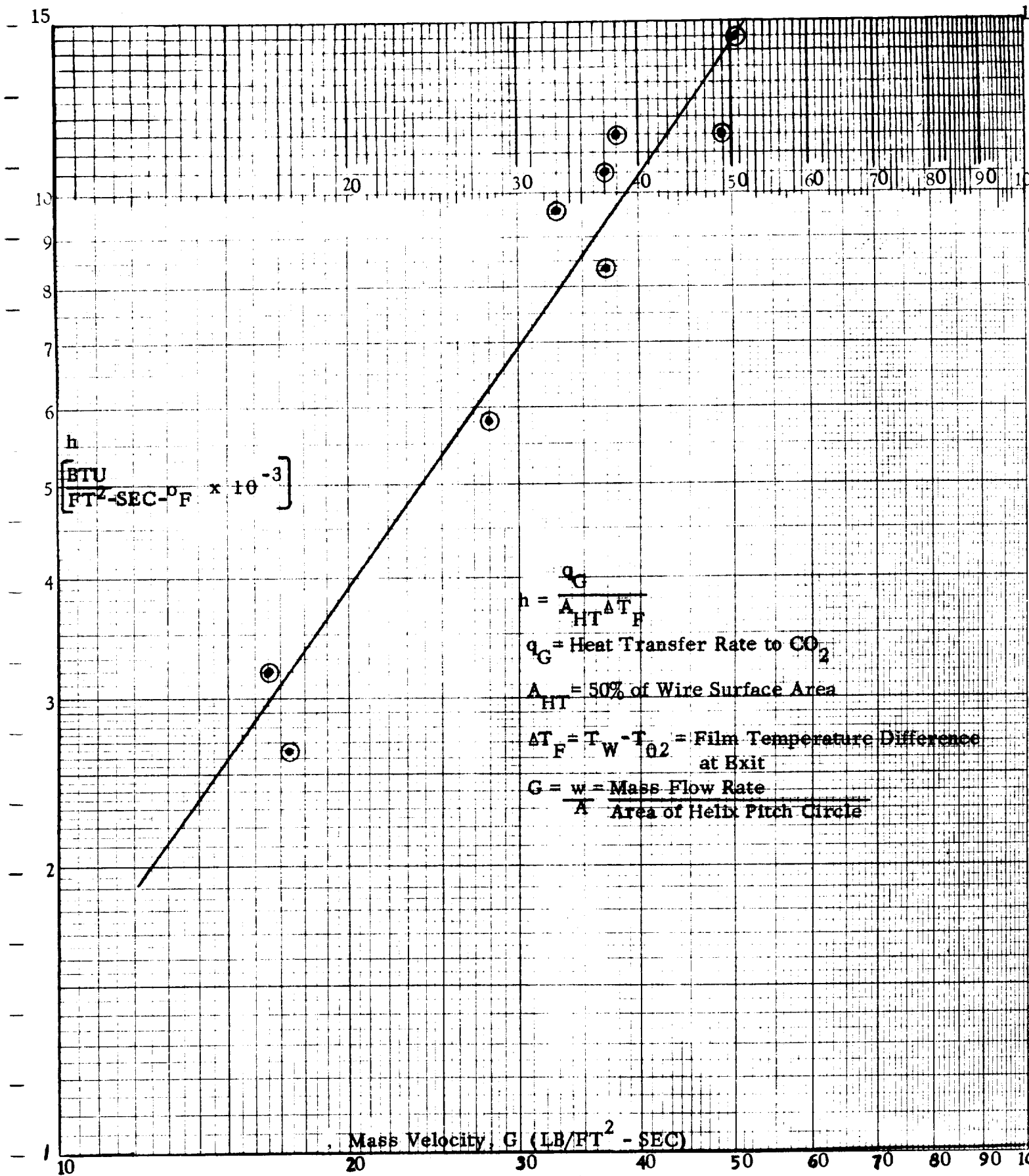
where the effective heat transfer area (A_{HT}) is assumed to be one-half the surface area of the helical Nichrome heater wire and the film temperature difference (ΔT_F) is the difference between the measured maximum wire temperature (near the nozzle end) and the measured gas exit temperature.

Calculated values of the mass flow rate, electrical efficiency and heat transfer coefficient are tabulated in Table V-1.

The values of electrical efficiency vary from 25 per cent to 55 per cent over the range of measurements which does not extend to an inlet pressure of 150 psia and power input of 2000 watts for which the unit was originally designed.

The experimental data show that the heat transfer area should be increased substantially in order to obtain the desired gas exit temperature near 1600° F. Based on the maximum measured gas discharge temperature of 555° F. in these experiments, the specific impulse for expansion to a vacuum with a large area ratio nozzle would be approximately 90 seconds. However, it appears to be feasible to attain values of specific impulse with CO₂ of at least 110 seconds by proper design of the heat exchanger.

The heat transfer coefficients were correlated as shown in Figure V-8 by plotting against the mass velocity G, which is defined as the mass flow rate divided by the area of the pitch circle of the helical Nichrome heater. The data show some scatter and appear to vary somewhat more rapidly than the first power of mass velocity within the range of measurements. However, the correlation appears quite good considering the accuracy of wall temperature measurements ($\pm 100^\circ$ F.) and the fact that no corrections have been introduced for variations in Prandtl number or viscosity of CO₂ or for large differences between wall and gas temperatures.



HEAT TRANSFER COEFFICIENT vs. MASS VELOCITY FOR OHMJET HELICAL HEATER

FIGURE V-8

VI - CONCLUSIONS

1. For a typical 150 ft. diameter rotating manned space station, it has been found that the angular impulse requirements to compensate for gravity gradient torques substantially exceed the angular impulse required to precess the spinning station at a rate of 360° per year to maintain sun orientation.
2. The secular gravity gradient torque is the predominant disturbing torque and it is periodic, with a period of approximately 54 days, depending on the regression rate of the orbit. In a typical worst case, the secular gravity gradient torque, if uncorrected, could misalign a station by 0.3° per orbit or 4.8° per day.
3. The periodic component of gravity gradient torque which averages to zero over each orbit, typically produces an angular deviation of the station axis of less than 0.115° which can generally be ignored unless rigid requirements on sun orientation accuracy were imposed.
4. Corrections for gravity gradient torque can be made by applying a short duration (1 to 5 sec.) thrust impulse either toward the sun or away from the sun at the proper point near the station periphery once each station rotation or very Nth rotation during all or a part of each orbit. The mean angular position of the thrust device during its firing, as measured in the plane of rotation, and the net impulse delivered per orbit should be controlled and changed gradually over the 54 day cycle of secular gravity gradient torque in order to minimize propellant consumption. In this way the corrective impulse can be applied with the maximum moment arm around the desired axis for the corrective torque and the net impulse delivered per orbit can be modulated to avoid over-compensation for gravity gradient torque.
5. Design studies of the Ohmjet electrically-heated pulse rocket system and the Heliojet solar-heated pulse rocket system indicate that all the thrust requirements for gravity gradient torque compensation, annual precession, and orbit maintenance can be accomplished using as propellant the carbon dioxide generated by the crew if the CO_2 is heated to approximately 1600° F. to increase the specific impulse to a value near 120 seconds.

7. Design studies of the Heliojet solar heated pulse rocket system show that two thrust units, each having a solar collector diameter of approximately two feet, could accomplish attitude control and orbit maintenance of a 150 ft. diameter space station. The system should use a CO₂ recovery and storage system to permit operation of the Heliojet every one or two station rotations while it is in sunlight. If the Heliojet were designed to operate only for a few minutes per orbit during regeneration of molecular sieve beds (which would have to occur in sunlight) the solar collector size required would become excessive.
8. The weight of a complete Heliojet system, including CO₂ recovery and storage equipment but excluding the weight of CO₂ consumed, is estimated to be approximately 138 lbs. as compared to 335 lbs. for an Ohmjet system which uses CO₂ directly from molecular sieve beds and 411 lbs. for an Ohmjet system which uses CO₂ compressors and storage tanks. Over 60 per cent of an Ohmjet system weight is associated with the increased weight of the auxiliary electric power system required. For comparison, the weight of a chemical thrust system ($I_{sp} = 300$ sec.) is estimated to be about 7500 lbs. for a one year life.
9. Tests of an Ohmjet thrust unit with pulsed operation at inlet pressures of 125 to 150 psig have demonstrated thrust levels of 0.31 to 0.375 lbs. with accurate control of pulse duration and with repeatability of the impulse delivered per pulse within the accuracy of the thrust measuring instrumentation ($\sim 5\%$).
10. Steady state tests of an Ohmjet thrust unit at inlet pressures up to 105 psia and power levels up to 1565 watts resulted in gas discharge temperatures up to 555° F., indicating that the heat transfer area would have to be increased to attain an outlet temperature of 1600° F. However, steady state electrical efficiencies up to 55 per cent were attained with no external thermal insulation on the Ohmjet unit. It appears that specific impulse values of at least 110 seconds with CO₂ should be attainable with an improved heat exchanger design.
11. Heat transfer coefficients were measured for the Ohmjet unit which would permit a more accurate analysis to optimize the design.

VII - RECOMMENDATIONS

1. In view of the advantages in simplicity and potential reliability of an Ohmjet system which uses waste CO_2 directly from a molecular sieve bed, it is recommended that Ohmjet thrust units be designed to operate at low inlet pressures near one atmosphere and that experiments be conducted to determine the electrical and thermodynamic performance which is attainable under such conditions.
2. Additional analytical effort and computer studies should be conducted to determine whether there may be optimum orbits (launch date and time of day of launch) which would minimize the propellant required for gravity gradient torque compensation on space stations for a desired mission duration.
3. Analytical and design effort should be directed toward specifying design criteria for a space station attitude control system which incorporates a gravity gradient computer to minimize propellant consumption.
4. Because of the potential weight saving by using solar power instead of electrical power to heat an attitude control propellant, it is recommended that additional design and development work be conducted to obtain a more accurate evaluation of the potential of a Heliojet attitude control system. Studies indicate that a Heliojet should operate at low pressures to simplify or eliminate the problem of CO_2 compression and storage. In case the compressor can be eliminated, the time for molecular sieve bed regeneration should be increased so that CO_2 can be used directly from sieve beds during a large fraction of the time in sunlight, thereby minimizing solar collector size.

VIII - REFERENCES

- II - 1 Suddath, J. H., "A Theoretical Study of the Angular Motions of Spinning Bodies in Space, NASA TR R-83, 1960.
- II-2 Sissenwine, N., et al, "A Preview of the U. S. Standard Atmosphere, 1962", ARS Paper 2678-62 presented at the 17th Annual Meeting, Nov. 13-18, 1962, Los Angeles, California.
- II-3 Harris and Priester, Journal of Atmospheric Sciences, 19, pp.286-301, July 1962.
- II-4 Schalkowsky, S. and Cooley, W. C., "Gravity Gradient Torques on a Sun-Oriented Space Station", Exotech Incorporated Report TR-001, December 20, 1962.
- II-5 Thomson, W. T., "Introduction to Space Dynamics", John Wiley and Sons, New York, 1961.
- IV-1 Stephens, C. W. and Hare, Q. M., "Internal Design Considerations for Cavity Type Solar Absorbers", ARS Journal, Vol. 31, No. 7, July 1961, p. 896.
- IV-2 Wing, L. O. and Cameron, K. E., "Solar Collectors for use in Thermionic Power Supply Systems in Space", ARS Journal, Vol. 31, No. 3, March 1961, p. 327.

APPENDIX A

TRANSIENT HEAT TRANSFER ANALYSIS OF THE HELIOJET

I. Derivation of Equations -

The differential equations governing the Heliojet tube wall and gas temperatures are derived from appropriate energy balance equations for a differential section. An approximate solution is obtained which identifies the significant dimensionless parameters and serves as a guide in selecting the preliminary design.

A. General Assumptions

1. The tube wall is initially heated externally by solar radiation to a uniform temperature, T_{wo} , with no gas flow through the tube.
2. The duration of gas flow is short so that heat received through the wall from additional solar radiation during the gas flow pulse is negligible.
3. The tube wall is thin so that axial conduction in the wall may be neglected during gas flow and radial temperature variations across the tube wall may be neglected.
4. The gas flow is essentially incompressible at constant flow rate and with a constant heat transfer coefficient.
5. The radius of curvature of the tube center line is large compared with tube radius so the flow may be analyzed on the basis of one dimensional flow in a straight tube.
6. The flow is quasi-static; hence the gas temperature variation with distance along the tube may be found as a steady-state distribution corresponding to the instantaneous wall temperature.

B. Nomenclature

A	= tube cross-sectional area $\frac{\pi}{4}D^2$	ft ²
C _{pg} , C _{pw}	= specific heats for gas and wall	BTU/lb ^o F.
D	= tube diameter	ft
G	= gas mass velocity (=ρV)	lb/ft ² sec
h	= convection heat transfer coefficient	BTU/ft ² sec ^o F

$$K_1 = 4 \left(\frac{h}{C_{pg} G} \right) \left(\frac{1}{D} \right) = 4 \text{ St} \left(\frac{1}{D} \right) \quad \text{ft}^{-1}$$

$$K_2 = K_1 L$$

$$K_3 = \frac{h}{\delta \rho_w C_{pw}} = \text{St} \left(\frac{C_{pg}}{C_{pw}} \right) \left(\frac{G}{\rho_w \delta} \right) \quad \text{sec}^{-1}$$

$$K_4 = \left[\frac{1 - e^{-K_2}}{K_2} \right] K_3 \quad \text{sec}^{-1}$$

$$L = \text{tube length} \quad \text{ft}$$

$$\text{St} = \text{Stanton Number} = \frac{h}{C_{pg} G} \quad \text{—}$$

$$t = \text{time} \quad \text{sec}$$

$$T_g, T_{ge}, T_{gi} = \text{gas temperature at any point, at exit, at inlet} \quad \text{°F}$$

$$T_{ga} = \text{gas temperature averaged over tube length} \quad \text{°F}$$

$$T_w, T_{wa}, T_{wo} = \text{wall temperature at any point, averaged over tube length, initial uniform temperature} \quad \text{°F}$$

$$V = \text{gas velocity} \quad \text{ft/sec}$$

$$w = \text{weight flow rate of gas} \quad \text{lb/sec}$$

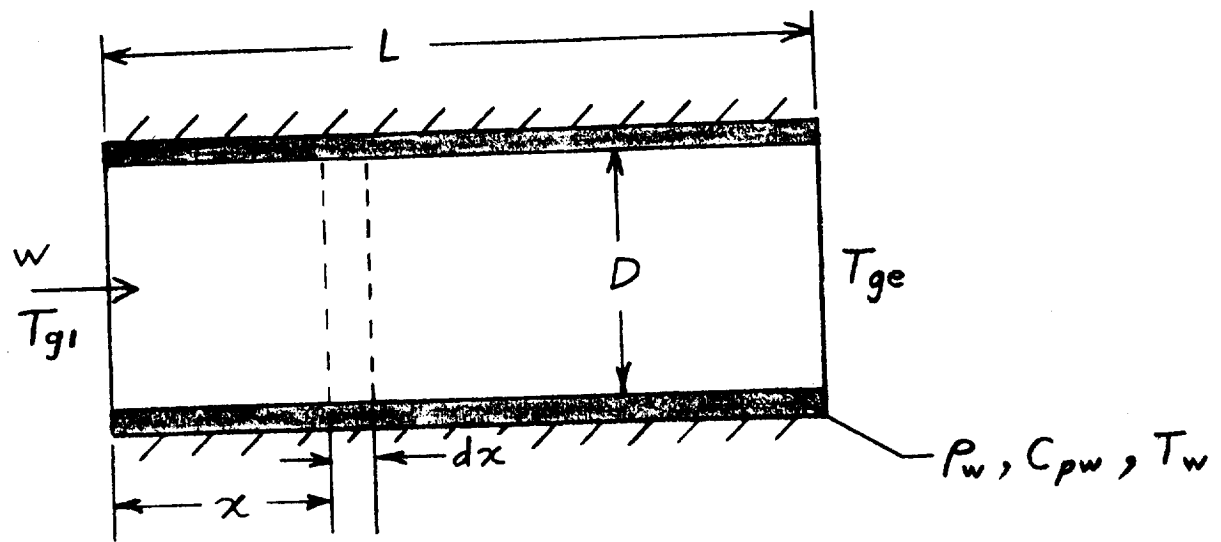
$$x = \text{distance along tube from inlet} \quad \text{ft}$$

$$\delta = \text{tube wall thickness} \quad \text{ft}$$

$$\rho_g, \rho_w = \text{weight density of gas, tube wall material} \quad \text{lb/ft}^3$$

C. Heat Balance Equations

In view of assumptions 2, 3, and 5 the heat exchanger tube is treated as an externally insulated straight tube with wall temperature as a function of x and t as shown in Figure A-1.



TUBE GEOMETRY FOR HEAT TRANSFER ANALYSIS

FIGURE A-1

A unit mass of gas moving a distance dx in unit time acquires from the wall thermal energy equal to $C_{pg} dT_g$; hence for $w = \rho_g VA = GA$ the heat balance equation is:

$$G \frac{\pi}{4} D^2 C_{pg} dT_g = h \pi D dx (T_w - T_g)$$

$$dT_g = \frac{4 h dx}{C_{pg} DG} (T_w - T_g) \quad (1)$$

Dividing by dt and using:

$$\frac{dx}{dt} = V, \quad \frac{dT_g}{dt} = \frac{\partial T_g}{\partial t} + \vec{w} \cdot \vec{\nabla} T = \frac{\partial T_g}{\partial t} + \frac{\partial T_g}{\partial x} V$$

we get:

$$\frac{1}{V} \frac{\partial T_g}{\partial t} + \frac{\partial T_g}{\partial x} = \frac{4 h}{C_{pg} DG} (T_w - T_g) \quad (2)$$

Consider next the heat loss from the wall which equals the rate of decrease of stored energy in the wall, i.e.:

$$\rho_w C_{pw} \pi D dx \frac{\partial T_w}{\partial t} = -h \pi D dx (T_w - T_g)$$

$$\frac{\partial T_w}{\partial t} = -\frac{h}{\rho_w C_{pw}} (T_w - T_g) \quad (3)$$

Equations (2) and (3) must be solved simultaneously subject to the boundary conditions:

$$\begin{aligned} \text{at } t = 0: T_w(x, 0) &= T_{w0} = \text{const.} \\ \text{at } t = 0: T_g(0, t) &= T_{g1} = \text{const.} \end{aligned} \quad (4)$$

In view of the quasi-static assumption, 6:

$$\frac{1}{V} \frac{\partial T_g}{\partial t} \ll \frac{\partial T_g}{\partial x}$$

and the two equations to be solved may be written as:

$$\frac{\partial T_g}{\partial x} = K_1 (T_w - T_g) \quad (5)$$

$$\frac{\partial T_w}{\partial t} = -K_3 (T_w - T_g) \quad (6)$$

The Stanton number, which is defined to be (h/C_{pg}) is assumed to be given by the empirical correlation:

$$St = \frac{h}{C_{pg}} = 0.023 Re^{-0.2} Pr^{-0.6}$$

where Re = Reynolds number

Pr = Prandtl number

This equation is used to compute the heat transfer coefficient, h , for flow of CO_2 inside tubes. The effect of the film temperature difference on the heat transfer coefficient has not been included for this first order analysis.

II. Solution of Equations -

An upper limit for exit temperature, T_{ge} at $t = 0$ may be obtained by using the initial wall temperature T_{w0} in place of T_w in (5). The upper limit for T_{ge} may then be found by solving (6) with $T_g = T_{ge}(0)$ and using this value of $T_w(t)$ in (5). The result of such an approach is:

$$\frac{\Delta T_{ge \max}}{T_{ge}(t) - T_{g1}} = \frac{T_{w0} - T_{g1}}{T_{w0} - T_{g1}} = 1 - e^{-K_2} \left[1 + (1 - e^{-K_2}) (1 - e^{-K_3 t}) \right] \quad (7)$$

where: $K_2 = K_1 L$

This solution gives a reasonable value of $T_{ge}(0)$, assuming that the starting transient is short and wall temperature does not drop appreciably during this transient. However, equation (7) yields too high a gas exit temperature at $t = \infty$.

A probable lower limit may be obtained by solving (6) with $T_g = T_{g1}$, the inlet temperature instead of the exit temperature as above. For this case the result is:

$$\frac{\Delta T_{ge \min}(t)}{T_{wo} - T_{g1}} = \frac{T_{ge \min}(t) - T_{g1}}{T_{wo} - T_{g1}} = (1 - e^{-K_2 t}) e^{-K_3 t} \quad (9)$$

This solution starts ($t = 0$) at the same point as the maximum limit case, but falls off too rapidly to the proper final value of $T_{ge}(\infty) = T_{g1}$.

A much better estimate of $T_{ge}(t)$ lying between the two limits above may be made by using average values for the temperature in solving (5) and (6). This solution is worked out in detail below.

In equation (5) use $T_w = \frac{1}{L} \int_0^L T_w dx$, i.e. the heat flux is based upon an average wall temperature instead of the extreme case ($T_w = T_{wo}$) as in the previous solutions.

$$\frac{\partial T_g}{\partial x} = K_1 (T_{wa} - T_g) \quad (10)$$

Equation (10) has the solution:

$$T_g(x, t) = T_{wa}(t) - [T_{wa}(t) - T_{g1}] e^{-K_1 x} \quad (11)$$

where: at $x = 0$: $T_g(0, t) = T_{g1}$ = inlet temperature

at $x = \infty$: $T_g(\infty, t) = T_{wa}$ = average wall temperature.

Equation (6), if averaged over L is:

$$\frac{\partial T_{wo}}{\partial t} = -K_3 (T_{wa} - T_{ga}) \quad (12)$$

From (11) we have:

$$T_{ga}(t) = \frac{1}{L} \int_0^L T_g(x, t) dx = T_{wa}(t) - \frac{1}{K_2} (1 - e^{-K_2}) [T_{wa}(t) - T_{g1}] \quad (13)$$

Substituting into (12) we get:

$$\frac{dT_{wa}}{dt} + \frac{K_3}{K_2} \left(1 - e^{-K_2} \right) T_{wa} = \frac{K_3}{K_2} \left(1 - e^{-K_2} \right) T_{g1} \quad (14)$$

with solution:

$$T_{wa}(t) = T_{g1} + (T_{wo} - T_{g1}) e^{-K_4 t} \quad (15)$$

$$\text{where: } K_4 = \frac{K_3}{K_2} \left(1 - e^{-K_2} \right) \quad (16)$$

at $t = 0$: $T_{wa}(0) = T_{wo}$ = initial wall temperature

at $t = \infty$: $T_{wa}(\infty) = T_{g1}$ = inlet gas temperature

We now substitute (15) into (11) to get:

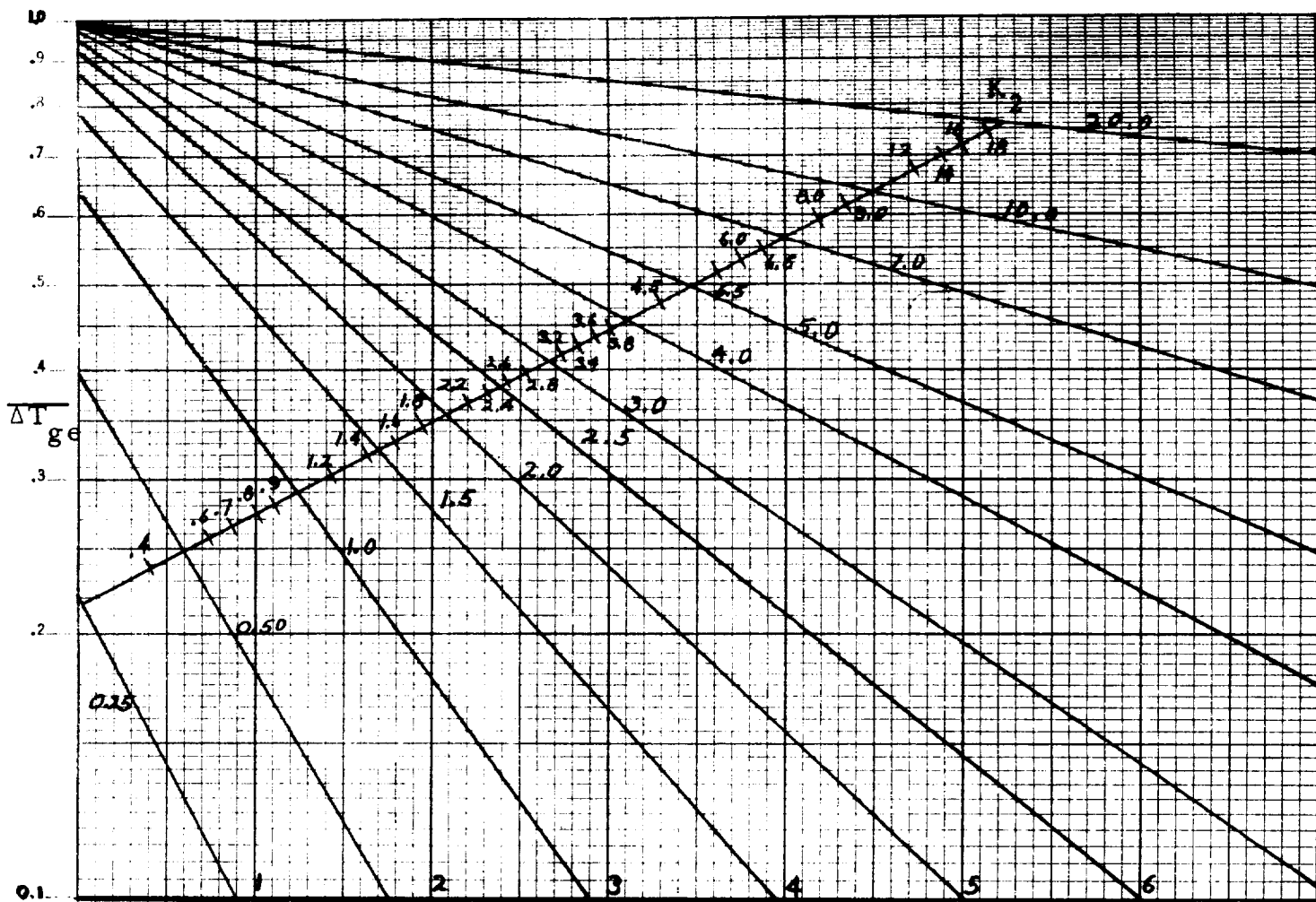
$$T_g(x, t) = T_{g1} + (T_{wo} - T_{g1}) \left(1 - e^{-K_1 x} \right) e^{-K_4 t} \quad (17)$$

which checks all the initial and final conditions. The exit temperature is accordingly:

$$\frac{\Delta T_{ge}}{\Delta T_{ge}} = \frac{T_{ge}(t) - T_{g1}}{T_{wo} - T_{g1}} = \left(1 - e^{-K_2} \right) e^{-K_4 t} \quad (18)$$

Repeated iterations do not change (17); hence, the answer is the best possible based on the assumption that the wall is isothermal at each instant of time. Equation (18) is plotted in Figure A-2. The average wall temperature for equation (15) is shown in Figure A-3. A comparison of all solutions for the special case $K_2 = 3.0$ is given in Figure A-4.

Exact analytical solutions for equations (5) and (6) which have been found by the use of Laplace transforms are too unwieldy for easy use.



$$\frac{\Delta T_{ge}}{T_{ge}(t) - T_{gl}} = \frac{T_{gl} - T_{w0}}{T_{gl} - T_{w0}} = (1 - e^{-K_2 t}) e^{-K_4 t}$$

$T_{ge}(t)$ = Exit Temperature, degrees F.

T_{gl} = Inlet Temperature, degrees F.

T_{w0} = Tube Wall Initial Temperature, degrees F.

$$K_2 = 4 \frac{h}{G_{pg} G D} = 4 St \frac{1}{D}$$

G = Area Flow Rate; # / Ft² Sec

$$K_4 = \frac{1 - e^{-K_2}}{K_2} K_3; \text{Sec}^{-1}$$

ρ_w = Tube Density; # / Ft³

$$K_3 = \frac{h}{\rho_w \delta C_{pw}} = St \frac{C_{pg}}{C_{pw}} \frac{G}{\rho_w \delta}; \text{Sec}^{-1}$$

t = Flow Duration; Sec

h = Heat Transfer Coefficient; BTU / Ft² Sec⁰ F.

C_{pg}, C_{pw} = Specific Heats of Gas, Wall; BTU / # °F.

St = Stanton Number $\left[0.023 \left(\frac{GD}{\mu} \right)^{-0.2} \left(\frac{\mu C_{pg}}{k} \right)^{-0.6} \right]$

HELIOJET GAS EXIT TEMPERATURE VARIATION WITH TIME

FIGURE A - 2

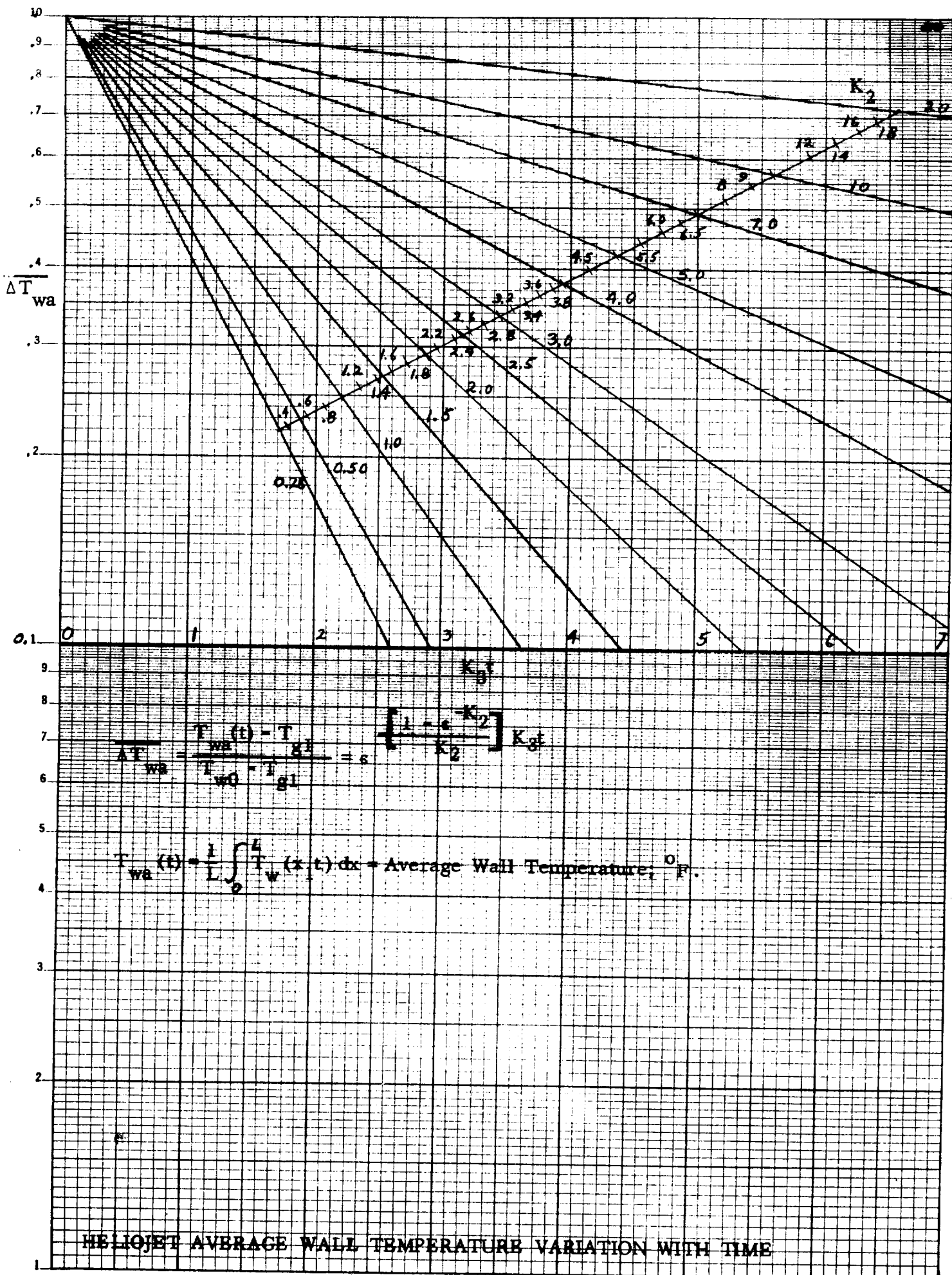


FIGURE A - 3

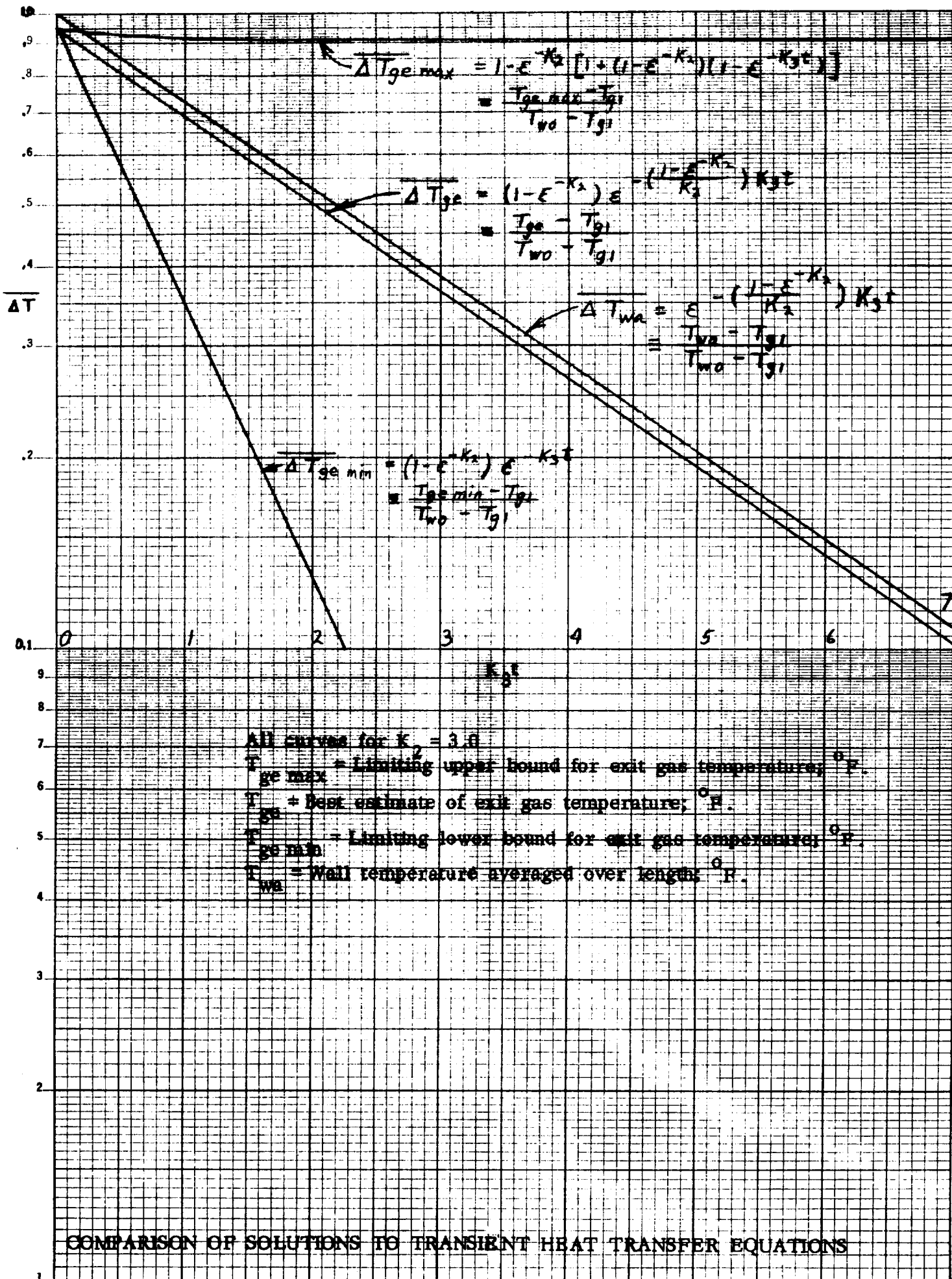


FIGURE A - 4